Submitted to Nuclear Physics

LBL-206
Preprint c.2

SHELL MODEL CALCULATIONS OF FISSION DECAY WIDTHS AND PROBABILITIES IN SUPERHEAVY NUCLEI

L. G. Moretto

July 1971

AEC Contract No. W-7405-eng-48

TWO-WEEK LOAN COPY

This is a Library Circulating Copy
which may be borrowed for two weeks.
For a personal retention copy, call
Tech. Info. Division, Ext. 5545

LBL-206

34

DISCLAIMER

This document was prepared as an account of work sponsored by the United States Government. While this document is believed to contain correct information, neither the United States Government nor any agency thereof, nor the Regents of the University of California, nor any of their employees, makes any warranty, express or implied, or assumes any legal responsibility for the accuracy, completeness, or usefulness of any information, apparatus, product, or process disclosed, or represents that its use would not infringe privately owned rights. Reference herein to any specific commercial product, process, or service by its trade name, trademark, manufacturer, or otherwise, does not necessarily constitute or imply its endorsement, recommendation, or favoring by the United States Government or any agency thereof, or the Regents of the University of California. The views and opinions of authors expressed herein do not necessarily state or reflect those of the United States Government or any agency thereof or the Regents of the University of California.

SHELL MODEL CALCULATIONS OF FISSION DECAY WIDTHS AND PROBABILITIES IN SUPERHEAVY NUCLEI†

L. G. Moretto

Lawrence Berkeley Laboratory
University of California
Berkeley, California 94720

July 1971

Abstract

The stability of excited superheavy nuclei with respect to fission is studied on the basis of realistic shell models and of the B.C.S. Hamiltonian. A statistical approach is used to calculate the deformation probabilities of excited nuclei as well as the fission and neutron decay widths. The results of the calculations show a rapid washing out with energy of the shell effects responsible for the high fission barriers predicted in the superheavy region. The first chance fission probabilities are calculated for nuclei is the region between Z = 108 and Z = 126. Two single-particle models proposed by Nilsson and by Bolsterli *et al*. have been used in the calculations. The results are discussed in terms of the possible production of superheavy elements by means of standard nuclear reactions.

†Work performed under the auspices of the U. S. Atomic Energy Commission and supported in part by Centro di Radiochimica e Analisi per Attivazione, Università di Pavia, Italy.

1. Introduction

Shell model calculations have led to the expectation that magic or near magic regions exist close to Z = 114 and N = 184. Shell closures are known to produce nuclear binding energies substantially larger than average: furthermore such potential energy depressions are limited to spherical or near spherical configurations. On this basis it was expected that the presence of such shells would generate substantial fission barriers in a region where the liquid drop model predicts insignificant barriers. The main mode of instability for very high Z elements is spontaneous fission: the presence of magic or near magic regions would allow for substantial fission barriers, thus increasing the spontaneous fission half lives.

Such considerations have led to a great amount of theoretical study on the stability of superheavy elements[1,2,3,4]) and also to the attempt of synthesizing them by means of nuclear reactions[5,6]) or to find them in nature[5,7,8,9] but with inconclusive results.

The theoretical studies carried on so far concerned the nuclear potential energy surface as a function of one or more deformation parameters. Such potential energies are calculated usually by means of the so-called Strutinski[10]) procedure. The use of the shell model as such for the calculation of the nuclear binding energy, while accounting reasonably well for the fluctuations due to the shells, leads to erroneous absolute values. The Strutinski procedure subtracts from the overall energy calculated by means of the shell model, a suitably smoothed energy, obtained from the model itself. The fluctuations or wiggles obtained in this way are then added to the liquid drop energy which provides a satisfactory smooth value for the overall binding energy.

In this way the nuclear potential energy can be described reasonably well and equilibrium deformations, masses, fission barriers, alpha and beta decay energies can be predicted.

The application of such a method to the superheavy nuclei has led to impressive predictions such as fission barriers of 8 or 9 MeV and large overall decay half lives in many cases[2,3]). For comparison ^{232}Th and ^{238}U have fission barriers of about 6 MeV while the other actinides have even lower fission barriers.

The analysis of the potential energies alone does not allow one to draw definite conclusion regarding the actual possibility of making such superheavy elements. Two more problems must be studied. The first concerns the actual possibility of obtaining suitable compound nuclei: since substantially large projectiles are needed in order to reach the magic region, there is some doubt whether complete fusion of target and projectile with a subsequent relaxation of the system to the compount nuclear stage is indeed possible. This point has been discussed by W. Swiatecki[11]). The second problem, which is the subject of the present paper, concerns the attenuation of the shell effects with excitation energy. As it has been mentioned above, shell effects are responsible for the large predicted fission barriers: the excitation energy, by depleting the lower shell of nucleons and by populating the higher one, tends to introduce a smearing of the shell effects. Such an effect is improperly considered a reduction of the fission barrier height with increasing excitation energy. In treating the present subject, a thermodynamical or a statistical approach is more appropriate and penetrating. If the system were at constant temperature, one could simply substitute the free energy for the potential energy; the free energy, just as the potential energy, has the property of being

at a minimum for equilibrium configurations. Such a potential would account for the warming up of the nucleus with the consequent smearing of shell effects. However, a compound nucleus, particularly when large excursions from equilibrium deformations are involved, can hardly be considered at constant temperature. Actually, the compound nucleus is at a fixed excitation energy and consequently the proper thermodynamical function to use is the entropy. At each excitation energy, one should study the variation of entropy with deformation or, in the language of statistical mechanics, the variation of the statistical probability with deformation. All the information required regarding the washing out of shell effects will be included in such functions.

In the present paper, a theory will be illustrated which allows one to calculate the statistical probability associated with deformation, the location of the fission transition state, the fission width and the fission probability on the basis of the shell model. Furthermore, the theoretical models necessary for such calculations will be presented. Finally, actual calculations will be presented for some superheavy nuclei ranging from Z = 110 to Z = 126. In such calculations, two different shell models have been used.

Some preliminary results of such calculations were published elsewhere[12]).

2. Theoretical Considerations

2.1. Probability of Deformation

In previous papers[13,14]), a calculation of the statistical probability associated with a given deformation for an excited nucleus, was presented. The procedure is based upon the coupling of one or more collective modes of motion with the internal degrees of freedom, with the assumption that excitation energy is randomly shared between internal and collective degrees of freedom. The deformation probability at a given excitation energy turns out to be:

$$P(E, \varepsilon)\, d\varepsilon = \frac{\sqrt{2\pi m}}{h}\, A'^{-1/2}\, \rho(E_T)\, d\varepsilon \quad , \tag{1}$$

where ε is the collective coordinate, m is the inertial mass associated with it, $E_T = E - V(\varepsilon)$ is the local excitation energy at the deformation ε, $V(\varepsilon)$ is the potential energy, $\rho(E_T)$ is the level density due to internal degrees of freedom at the deformation ε and at the local excitation energy E_T and:

$$A' = \left(\frac{d\ \ln\rho}{d\ E}\right)_{E=E_T} \quad .$$

In such an expression, the leading term is $\rho(E_T)$: it accounts for essentially all of the fluctuations of probability as a function of deformation and it contains the feature of the shell smearing with excitation energy. Of much less significance is the inertial mass, which, although it depends both on excitation energy and deformation, has an insignificant effect on the relative probability. The potential energy $V(\varepsilon)$ is very relevant also, since it appears in the dependence of E_T upon E in the argument of the level density.

Actually, the success of the calculation depends on the ability to evaluate both the potential energy and the level density on the basis of a realistic nuclear model.

The expression given in eq. (1) is relevant to the fission process in so far as it can describe the probability of fluctuations in shape no matter how large. The fission process is indeed connected with a large fluctuation in shape, and its probability is related to the probability of such fluctuations. In the next section, such considerations will be treated quantitatively.

2.2. THE TRANSITION STATE IN FISSION

In the case of a non-fissioning and, in general, non-decaying compound nucleus, eq. (1) is a function approaching to zero at some large deformation ($P = 0$ for $E = V(\varepsilon)$) and with a finite integral over the deformation space. This integral is the overall level density of the nucleus at the excitation energy E. It can be said that the system is bound in the compound-nucleus deformation space. With a nucleus which can undergo fission, a new situation occurs: namely, along some direction in the deformation space, the probability does not ever go to zero; however, after going through a minimum, it increases dramatically for configurations farther and farther away from sphericity. Also the integral of the probability over the deformation space tends to diverge. In such a case, one cannot speak of statistical equilibrium in a true sense: it is better to think in terms of a bulk probability, contained within a deformation boundary which could be called the compound nucleus region and which leaks out through some special deformation configuration into the region where the fission fragments are formed. If the decay probability is small, the system

can be still considered quasi-bound in the compound nucleus configuration and the compound nucleus itself retains a physical significance. The special configuration which controls the flow of probability towards fission is the region where the probability itself is at a minimum and is called transition state.

Usually the transition state is considered to be located at the fission saddle point which is a point in the potential energy surface. However, such an identification is not necessarily correct when the fission barrier is primarily the result of shell effects rather than deriving from the liquid drop potential energy. Indeed the excitation energy will tend to wash out the shell effects, but such a washing out can take place at a different rate for different deformations. Therefore the minimum in probability (or the transition state) does not necessarily coincide in deformation with the saddle point at all excitation energies. It follows that in order to evaluate the fission widths and probabilities, one should search for the location of the transition state at all excitation energies. Similar considerations have been made by Ramamurthy et al.[16]).

2.3. FISSION DECAY WIDTHS AND PROBABILITIES

The fission width can be written as follows:

$$\Gamma_F = \frac{1}{2\pi\rho(E)} \int_0^{E_x} \rho(x, \varepsilon)\, dx$$

where $E_x = E - V(\varepsilon)$ and the coordinate ε takes its value where $P(E, \varepsilon)$ is at a minimum. The level density $\rho(E)$ refers to the compound nucleus. By recalling the exponential behaviour of the level density, one can write with very good approximation:

$$\Gamma_F = \frac{1}{2\pi\rho(E)} \quad \frac{1}{A'} \quad \rho(E_x, \varepsilon)$$

where

$$A' = \left(\frac{d\ \ln \rho(x)}{dx}\right)_{x=E_T}$$

This approximation shows clearly the simple relation between the fission width and the deformation probability at the transition state. It can also be seen that the fission width is independent of the inertial mass of the transition state.

Similarly, the neutron decay width is given by the relation:

$$\Gamma_N = \frac{1}{2\pi\rho(E)} \quad \frac{4\ m_N}{\pi\hbar^2} \int_0^{E-B_N} \sigma_{inv}\ \rho(x)\ (E - B_N - x)\ dx$$

where m_N is the neutron mass, σ_{inv} is the cross section for the inverse reaction and B_N is the neutron binding energy. The level density $\rho(E)$ refers again to the compound nucleus, while $\rho(x)$ refers to the residual nucleus after neutron emission.

Also, the neutron decay width can be written in an approximate and convenient form:

$$\Gamma_N = \frac{1}{2\pi\rho(E)} \times 0.18918\ A^{2/3}\ \frac{1}{A'^2}\ \rho(E - B_N)$$

where A is the mass number of the residual nucleus, $A' = \left(\frac{d\ \ln \rho(x)}{dx}\right)_{x=E-B_N}$ and the numerical constant is calculated on the assumption of constant inverse cross sections.

The first chance fission probability is:

$$P_F = \frac{\Gamma_F}{\Gamma_F + \Gamma_N}$$

assuming that fission and neutron emission are the only competing decay processes.

The first chance fission probability must not be confused with the total fission probability $\frac{\sigma_F}{\sigma_R}$. While the former accounts for the compound nucleus fission only, the latter includes all the fissions occurring along the whole neutron evaporation chain and in many cases, could be much larger than the first chance fission probability.

3. Models Employed in the Calculations

3.1. THE SHELL MODELS

Two different shell models have been employed in the present calculations. The first model, proposed by Bolsterli *et al.*[15]) contain the spin independent part of the single particle potential which is obtained by folding an effective two nucleon interaction with a uniform sharp-surface psuedo density. Such a form of the potential is very close to the Wood Saxon potential. In such a model the shape of the nucleus is specified by means of smoothly joined portions of three quadratic surfaces of revolution. The single particle energy levels and spins have been calculated for the nucleus $^{188}_{114}X$ and used without modification for the other nuclei close-by. The second model consists of a modified three dimensional harmonic oscillator potential proposed by Nilsson[2]): the shapes of the nucleus have been restricted to a family of ellipsoids of revolution. The values of the coupling parameters K and μ which have been used are:

	Protons	Neutrons
K	0.0534	0.0634
μ	0.686	0.256

These values are expected to be more suitable for A = 296. The calculations presented here extend below and above this mass number: no attempt has been made to modify the coupling parameters. The only A dependence in the calculation has been that introduced by the scaling quantity:

$$\hbar\omega_o^o = 41/A^{1/3}$$

3.2. CALCULATIONS OF THE FISSION BARRIERS

The potential energy of superheavy nuclei as a function of deformation has been calculated by means of a modified Strutinski procedure illustrated elsewhere[14]). The fission barriers obtained from the model proposed by Bolsterli *et al.* were taken from the same authors: such fission barriers for the nuclei $^{296}_{108}X$, $^{290}_{110}X$, $^{298}_{114}X$, and $^{296}_{116}X$ are shown in fig. 1. The fission barriers obtained from the Nilsson model have been calculated by us with the parameters specified in the previous sections. Only one deformation coordinate, the ellipsoidal deformation ε has been taken into account, since it has been shown that for superheavy nuclei the hexadecapole coordinate ε_4 is not particularly relevant up to the top of the fission barrier. The fission barriers of the nuclei $^{290}_{110}X$, $^{298}_{110}X$, $^{292}_{112}X$, $^{296}_{112}X$, $^{296}_{114}X$, $^{298}_{114}X$, $^{296}_{116}X$, $^{310}_{116}X$, $^{308}_{118}X$, $^{310}_{118}X$, $^{312}_{118}X$, $^{308}_{124}X$, $^{310}_{124}X$, $^{312}_{124}X$, $^{312}_{126}X$, $^{314}_{126}X$, $^{316}_{126}X$ are shown in fig. 2 through fig. 8 together with the liquid drop energies.

3.3. THE LEVEL DENSITIES

The level density formalism employed here has been described in detail in a previous paper[14]). The level densities are calculated on the basis of the actual sets of single particle levels at different deformations by means of a numerical procedure. The pairing effects are accounted for by means of the B.C.S. Hamiltonian which enters in the expression for the grand partition function used for evaluating the level density. Even-odd effects are allowed for by incrementing the ground state energy by the lowest-quasi-particle excitation associated to the odd nucleon. The complete consistency of the potential energies and of the level densities is to be stressed: both are based upon the same shell model levels and the same B.C.S. Hamiltonian is used

for the pairing effects. The level density calculations should be considered to be quite accurate and to contain a large amount of physical information without the introduction of any empirical constant. The washing out of the shell effects, which will be seen to occur with increasing excitation energy, is therefore a direct prediction of the single particle model. In fig. 9 two level density curves as a function of energy are shown: they refer to the same nucleus $^{296}_{116}X$ at sphericity and at the transition state deformation. It can be observed that the two level density curves behave so as to eliminate the effect of the 7 MeV difference in potential energy between the ground state and the saddle point. This point will be taken-up again in the discussion.

3.4. ACTUAL CALCULATIONS

The potential energy curves are first calculated as functions of deformations on the basis of a given shell model. The same shell model is then used for the level density calculations. The potential energies and the level densities are then used to obtain the deformation probabilities of the superheavy nuclei for a set of excitation energies as described in sec. 2.1. A quantity related to the deformation probability, namely $\ln P(E,\varepsilon)h/(2\pi m)^{1/2}$ is presented in fig. 10 through fig. 13 for the nuclei $^{296}_{108}X$, $^{290}_{110}X$, $^{298}_{114}X$, $^{296}_{116}X$ calculated on the basis of the shell model proposed by Bolsterli <u>et al</u>. and in fig. 14 and fig. 15 for the nuclei $^{290}_{110}X$ and $^{296}_{116}X$ on the basis of the Nilsson model.

At each excitation energy, the minimum in deformation probability (the transition state) is searched for and the deformation probability at the transition state is transformed into the fission decay width as described in sec. 2.3. Similarly the neutron decay width is calculated by using the level density

of the residual nucleus at its most probable deformation which in all the cases studied turned out to be sphericity. The neutron binding energies, necessary for the neutron decay width calculations have been taken from Nilsson et al.[2]) and are presented in Table 1 together with the fission barrier heights. The fission decay widths and the neutron decay widths are then used to evaluate the first-chance fission probabilities as a function of excitation energy. Such calculations have been performed for all the nuclei listed in sec. 3.2. The fission probabilities calculated from the Bolsterli et al. shell model are presented in fig. 16 and those calculated from the Nilsson shell model are presented in fig. 17 through fig. 23.

4. Discussion

The influence of the effects produced by the near magic regions close to Z = 114 and N = 184 can be evaluated by observing the actual potential energy curves in comparison with the liquid drop potential energies in fig. 1 through fig. 8. Only a small sample of nuclei have been considered here: a much larger survey has been made by Nilsson et al.[2]) and by Nix[3]) where calculated masses and half lives are also reported. A substantial number of such nuclei are predicted to have overall half lives sufficiently long to make them observable experimentally if they can be produced in their ground states. The conditions for reaching the ground states are, first, the compound nucleus formation through some suitable reaction, second the survival with respect to fission of the compound nucleus decay stage. It has been stressed in sec. 1 that the first point is very poorly known. As far as the second point is concerned it is possible now to give answers which should be as accurate as the potential energy calculations.

4.1. TEMPERATURE DEPENDENT SHELL EFFECTS

It was stated in sec. 1 that the excitation energy is expected to destroy the shell effects: this is particularly important in the case of superheavy nuclei whose stability against fission relies uniquely upon the shell effects. The primary shell effects are local deviations from uniformity in the single particle level density: such deviations affect the potential energy in the region close to the Fermi surface. Thermodynamical or statistical quantities are also influenced by the shell effects. The perturbations of the single-particle level density can be expanded in Fourier series. Gilbert[17]) has shown that a

perturbation with a wavelength λ is washed out by the temperature following the relation:

$$S \propto \exp(-2\pi^2 T/\lambda) \quad ,$$

where T is the temperature and S is the temperature dependent part of the shell effects as they influence some statistical quantity such as the entropy. The present calculations include such washing out automatically. A very striking example is the following. The nucleus $^{296}_{116}X$ has a fission barrier of $\sim$ 7.5 MeV and the location of the top of the barrier is at $\varepsilon = 0.225$ as can be observed in fig. 5. In fig. 9 the level densities are shown as a function of excitation energy for the same nucleus $^{296}_{116}X$ at the deformation $\varepsilon = 0$ and $\varepsilon = 0.225$. The level density at $\varepsilon = 0$ does not increase quite as fast as that at $\varepsilon = 0.225$: the value of the former at 20, 40, 60 MeV is equal to that of the latter at energies lower by 3.5, 6.0, 7.5 MeV respectively. This gives a rather accurate idea of the rate at which the shell effects are destroyed by the excitation energy. In this case the compound nucleus at 60 MeV excitation energy does not feel any shell effect whereas in the ground state it amounted to 7.5 MeV. In this sense it could be said that the nucleus at 60 MeV excitation energy does not have a relevant fission barrier any longer. A more general view of such effects is given by the deformation probability curves presented in fig. 10 through fig. 15. At low excitation energies the maximum probability is centered at sphericity; the higher this peak is the stronger the shell effects are. The compound nucleus region is limited by the transition state associated to the minimum in deformation probability. It should be pointed out that the portions of the curves beyond the transition state may be physically meaningless, since in such

regions the system is not expected to be at statistical equilibrium. With increasing excitation energy, the compound nucleus peaks tend to become decreasingly sharp while the deformation probability at the transition state increases substantially. At the highest excitation energies the compound nucleus peak is not visible any longer: only a more or less flat region in the deformation probability can be observed close to sphericity. Under such conditions the shell effects have essentially disappeared and the nucleus is left with only the liquid drop smooth potential energy: therefore it is quite doubtful whether one is justified in considering the existence of a compound nucleus at all.

4.2. FIRST-CHANCE FISSION PROBABILITIES

The first chance fission probabilities $P_F = \Gamma_F/(\Gamma_F + \Gamma_N)$ which are to be discussed are presented in fig. 16 through fig. 23. In order to have a frame of reference in the analysis of such quantities, it is worthwhile to consider an approximate expression for Γ_F/Γ_N obtained by assuming a uniform model in the level densities:

$$\frac{\Gamma_F}{\Gamma_N} \approx \frac{1}{0.19\ A^{2/3}}\ \frac{1}{T} \exp\left(\frac{B_N - B_F}{T}\right) \quad ,$$

where A is the compound nucleus mass number, B_N and B_F are the neutron binding energy and the fission barrier height respectively and T is the nuclear temperature. Such an expression can be obtained from the equations in sec. 2.3 for the high energy limit.

For a nucleus with $A \simeq 300$, the temperature $T \simeq 1$ MeV corresponds to an excitation energy between 30 and 40 MeV. In the case in which $B_F \simeq B_N$ the fission probability P_F given by the above expression is about 0.1. Similar calculations show that for $P_F = 0.5$, $B_N - B_F = 2.15$, for $P_F = 0.7$ $B_N - B_F = 2.98$ for $P_F = 0.8$ $B_N - B_F = 3.5$, for $P_F = 0.9$ $B_N - B_F = 6.35$. In all such cases the fission probability is expected to decrease very slowly with excitation energy.

A first inspection of the calculated first chance fission probabilities shows that for excitation energies of the order of 35 MeV and above, extremely high values are reached, up to ~ 0.95. Such high values would be predicted by the uniform model for neutron binding energies between 3 and 5 MeV larger than the fission barriers: since the neutron binding energies are of the order of 5 to 6 MeV this implies that, in order to obtain such fission probabilities the uniform model would require vanishingly small fission barriers. A check in Table 1 shows immediately that the true fission barriers are either very close to the neutron binding energies or even larger. It is then possible to say that, at sufficiently large excitation energies the calculated fission probabilities behave <u>as if</u> the nuclei under investigation had vanishingly small fission barriers. The question may arise why the washing out of the shell effects involves primarily the fission barriers and not the neutron binding energies. The answer is rather simple: although in superheavy nuclei the fission barriers arise because of shell effects, the neutron binding energies derive primarily from the liquid drop energy terms. Therefore the neutron binding energies are only slightly affected by the excitation energy. The low energy behavior of fission probabilities are instead to be considered normal in the sense that they reflect

to a large extent the actual values of the fission barriers. For fission barriers substantially larger than the neutron binding energies, the fission probabilities assume quite low values and increase rapidly with excitation energies. For fission barrier values smaller than the neutron binding energies, the fission probabilities assume rather large values which can sometimes fluctuate with increasing excitation energies depending upon the relative rate of increase of Γ_F and Γ_N.

4.3. STABILITY OF EXCITED SUPERHEAVY NUCLEI

Of course, the first chance fission probabilities alone do not indicate directly the overall probability for the compound nucleus to reach a ground state. The quantities which should be calculated are the total fission probabilities which take into account the probability of fission decay at every stage of the neutron evaporation cascase. Although the present calculations have been performed only for even even nuclei and therefore do not give sufficient information for the calculation of the overall fission probabilities more than one isotope corresponding to the same atomic number has been considered. Since such isotopes are very close to one another, an estimate of the chance of survival for a given compound nucleus can be obtained. The general conclusion is that the stability of the excited compound superheavy nuclei against fission is by far smaller than could be guessed on the basis of the fission barrier calculations. Only for a few cases does the probability of survival seem substantial and even then is significant only for relatively low excitation energies. However, if the formation of the superheavy compound nuclei is sufficiently likely, then the possibility that a detectable fraction of some compound nuclei will reach a ground state is not ruled out by the present calculations.

As a further remark it can be said that the present calculations have been carried out on the assumption that the single particle spectrum is independent on excitation energy. A self consistent calculation may show how good this approximation is. If, as it could be guessed, the excitation energy tends to smear out the single particle spectrum itself, then the present calculations represent a somewhat optimistic evaluation of the superheavy compound nucleus stability.

It should be mentioned that the present calculations do not account for the effect of the angular momentum on the fission barrier. Since angular momentum tends to decrease the fission barrier, the present estimates for the fission probabilities may be somewhat optimistic.

Acknowledgments

The author wishes to thank Prof. S. G. Nilsson for the helpful discussions and for the encouragement in the early stages of the work, Drs. C. F. Tsang and W. Swiatecki for their suggestions, and Dr. S. G. Thompson for the valuable corrections and comments on the manuscript.

References

1) Yu. A. Muzychka, V. V. Pashkevich, and V. M. Strutinski, Yad. Fiz. 8 (1960) 716

2) S. G. Nilsson, C. F. Tsang, A. Sobiczewski, Z. Szymanski, S. Wychech, G. Gustafson, I. L. Lamm, P. Moeller, and B. Nilsson, Nucl. Phys. A131 (1969) 1

3) J. R. Nix, LA-DC-12488, April 15, 1971

4) V. M. Strutinski, Nucl. Phys. A95 (1967) 420; A122 (1968) 1

5) S. G. Nilsson, S. G. Thompson, and C. F. Tsang, Phys. Lett. 28B (1969) 458

6) R. Bimbot, C. Deprun, D. Gardès, H. Gauvin, Y. Le Beyec, M. Lefort, J. Péter, and B. Tamain, preprint

7) P. B. Price, R. L. Fleischer, and R. T. Woods, Phys. Rev. C 1 (1970) 1819

8) E. Cheifetz, E. A. Giusti, H. R. Bowman, R. C. Jared, J. B. Hunter, and S. G. Thompson, in Proc. Int. Conf. on the Properties of Nuclei Far From the Region of Beta-Stability, Leysin, 1970 (CERN 70-30, Geneva, 1970), Vol. 2, p. 709

9) W. Grimm, G. Herrmann, and H. D. Schüssler, Phys. Rev. Lett. 26 (1971) 1040

10) V. M. Strutinski, Yad. Fiz. 3 (1966) 614; Sov. J. Nucl. Phys. 3 (1966) 448; Arkiv. Fysik 36 (1967) 629

11) W. J. Swiatecki, UCRL-19405

12) L. G. Moretto, Phys. Lett. 34B (1971) 191

13) L. G. Moretto and R. Stells, Phys. Lett. 32B (1970) 558

14) L. G. Moretto, LBL-228 (August 1971)

15) M. Bolsterli, E. O. Fizet, and J. R. Nix, in Proc. Second IAEA Symposium on Physics and Chemistry of Fission, Vienna, 1969 (International Atomic Energy Agency, Vienna, 1969) p. 183

16) V. S. Ramamurthy, S. S. Kapoor, and S. K. Kataria, Phys. Rev. Lett. 25 (1970) 386

17) A. Gilbert, Lawrence Berkeley Laboratory Report UCRL-18095 (June 1968)

Table 1. Neutron binding energies and fission barriers for superheavy nuclei.

	B_N(MeV)	B_F(MeV) (Bolsterli *et al.* model)	B_F(MeV) (Nilsson model)
$^{296}_{108}X$	4.57	2.80	
$^{290}_{110}X$	6.15	4.45	3.93
$^{298}_{110}X$	4.89		5.39
$^{292}_{112}X$	6.67		5.76
$^{296}_{112}X$	5.95		7.35
$^{296}_{114}X$	6.83		8.58
$^{298}_{114}X$	6.29	7.69	9.24
$^{296}_{116}X$	7.30	7.40	7.45
$^{310}_{116}X$	5.42		8.19
$^{308}_{118}X$	6.07		8.33
$^{310}_{118}X$	5.96		8.17
$^{312}_{118}X$	5.76		7.70
$^{308}_{124}X$	8.13		7.00
$^{310}_{124}X$	7.24		7.09
$^{312}_{124}X$	7.19		6.88

(continued)

Table 1 (continued)

	B_N(MeV)	B_F(MeV) (Bolsterli *et al.* model)	B_F(MeV) (Nilsson model)
$^{312}_{126}X$	7.57		6.14
$^{314}_{126}X$	7.51		5.83
$^{316}_{126}X$	7.36		5.79

Figure Captions

Fig. 1. Fission barriers for the nuclei $^{296}_{108}X$, $^{290}_{110}X$, $^{298}_{114}X$, and $^{296}_{116}X$ calculated on the basis of the shell model proposed by Bolsterli *et al.*[15]).

Fig. 2. Fission barriers for the nuclei $^{290}_{110}X$ and $^{298}_{110}X$ calculated on the basis of the Nilsson model[2]). The black dots represent the potential energies calculated by means of the Strutinski procedure; the solid line represents the liquid drop potential energy.

Fig. 3. Same as fig. 2 for the nuclei $^{292}_{112}X$ and $^{296}_{112}X$.

Fig. 4. Same as fig. 2 for the nuclei $^{296}_{114}X$ and $^{298}_{114}X$.

Fig. 5. Same as fig. 2 for the nuclei $^{296}_{116}X$ and $^{310}_{110}X$.

Fig. 6. Same as fig. 2 for the nuclei $^{308}_{118}X$, $^{310}_{118}X$, and $^{312}_{118}X$.

Fig. 7. Same as fig. 2 for the nuclei $^{308}_{124}X$, $^{310}_{124}X$, and $^{312}_{124}X$.

Fig. 8. Same as fig. 2 for the nuclei $^{312}_{126}X$, $^{314}_{126}X$, and $^{316}_{126}X$.

Fig. 9. Level densities for $^{296}_{116}X$ at the ground state and at the saddle-point deformation, respectively. The excitation energy is measured taking the local value of the potential energy as zero. The washing out of the 7.5 MeV difference in potential energy is visible at 60 MeV excitation energy.

Fig. 10. Deformation probabilities at different excitation energies for $^{296}_{108}X$ on the basis of the shell model proposed by Bolsterli *et al.* The deformation parameter y is defined in ref. [15]). The quantity $P(E,y)h/(2\pi m_y)^{1/2}$ has the dimension $MeV^{-1/2}$.

Fig. 11. Same as in fig. 10 for $^{290}_{110}X$.

Fig. 12. Same as in fig. 10 for $^{298}_{114}X$.

Fig. 13. Same as in fig. 10 for $^{296}_{116}X$.

Fig. 14. Same as in fig. 10 for $^{290}_{110}X$; the calculations have been performed on the basis of the Nilsson model.

Fig. 15. Same as in fig. 14 for $^{296}_{116}X$.

Fig. 16. First chance fission probabilities for $^{296}_{108}X$, $^{290}_{110}X$, $^{298}_{114}X$, $^{296}_{116}X$ on the basis of the shell model proposed by Bolsterli *et al*.

Fig. 17. First chance fission probabilities for $^{290}_{110}X$ and $^{298}_{110}X$ on the basis of the Nilsson model.

Fig. 18. Same as in fig. 17 for $^{292}_{112}X$ and $^{296}_{112}X$.

Fig. 19. Same as in fig. 17 for $^{296}_{114}X$ and $^{298}_{114}X$.

Fig. 20. Same as in fig. 17 for $^{296}_{116}X$ and $^{310}_{116}X$.

Fig. 21. Same as in fig. 17 for $^{308}_{118}X$, $^{310}_{118}X$, and $^{312}_{118}X$.

Fig. 22. Same as in fig. 17 for $^{308}_{124}X$, $^{310}_{124}X$, and $^{312}_{124}X$.

Fig. 23. Same as in fig. 17 for $^{312}_{120}X$, $^{314}_{126}X$, and $^{316}_{126}X$.

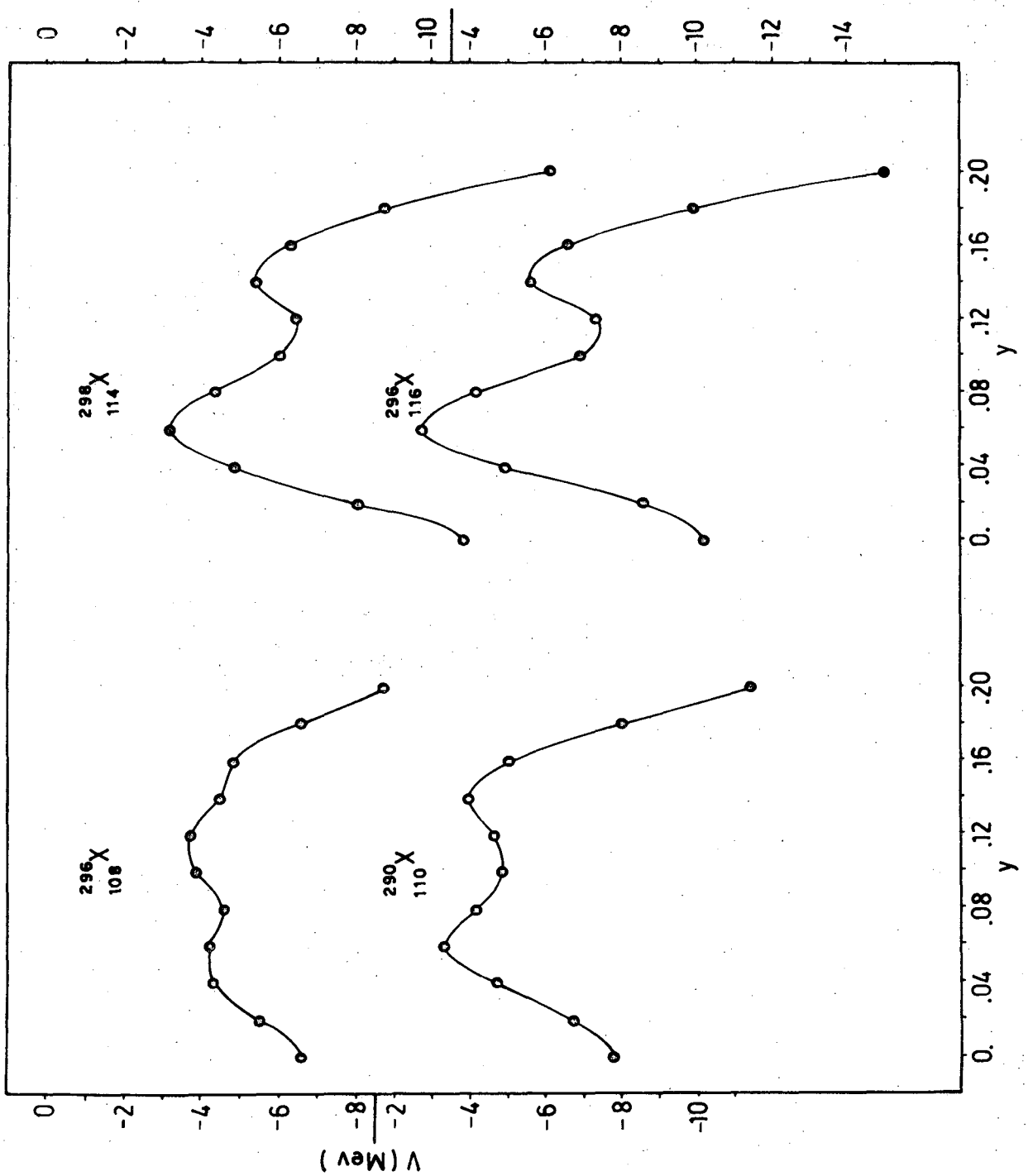

Fig. 1

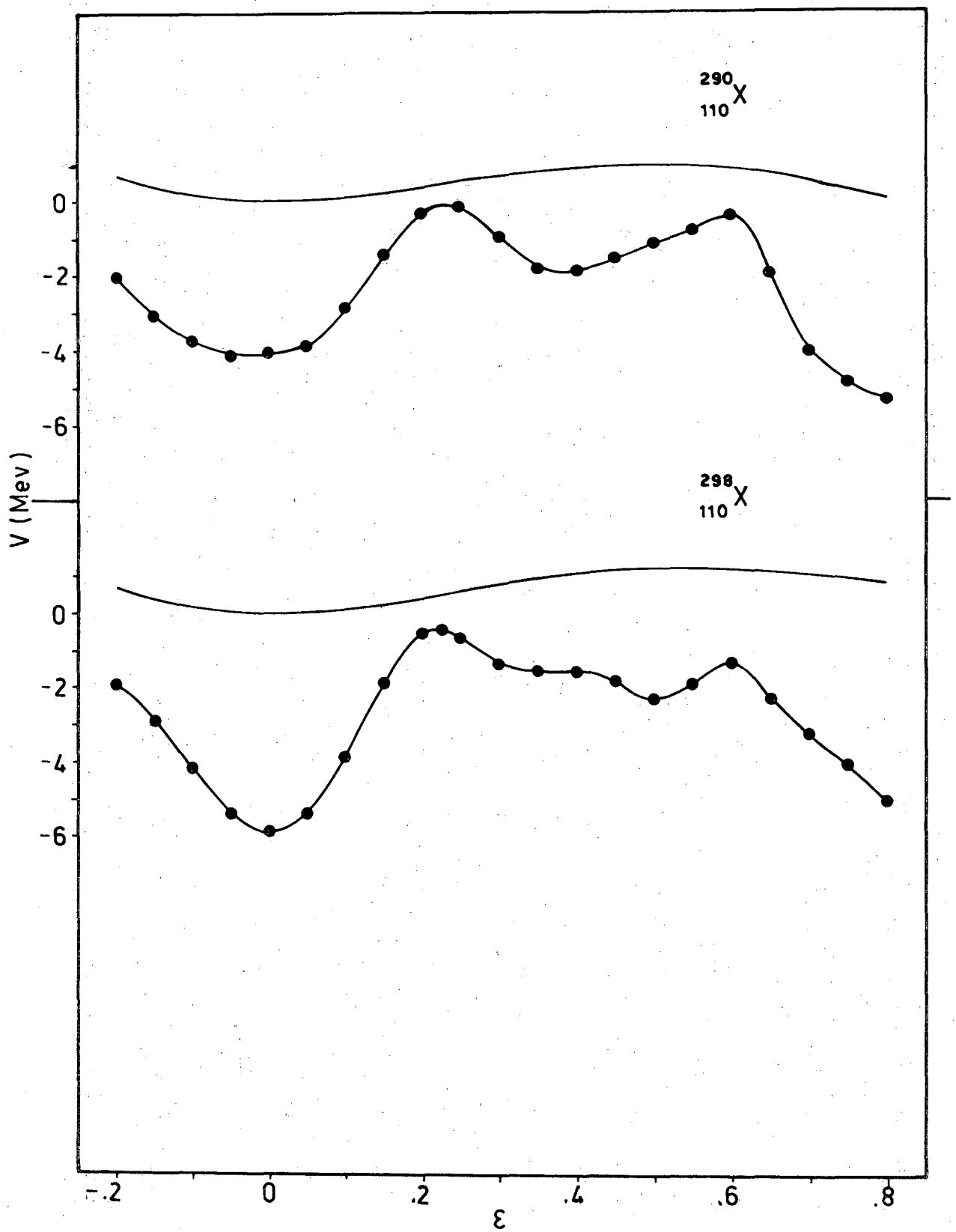

Fig. 2

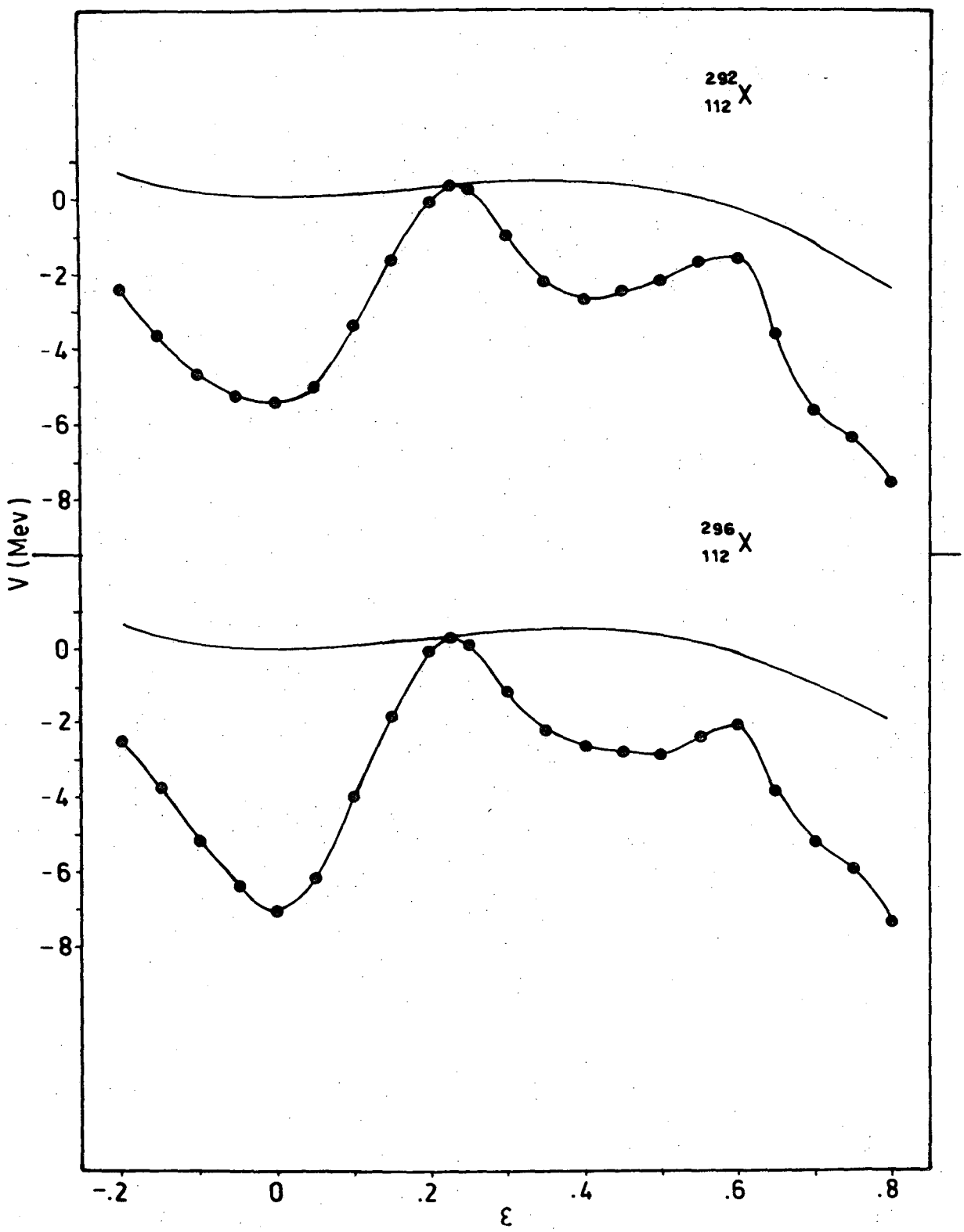

Fig. 3

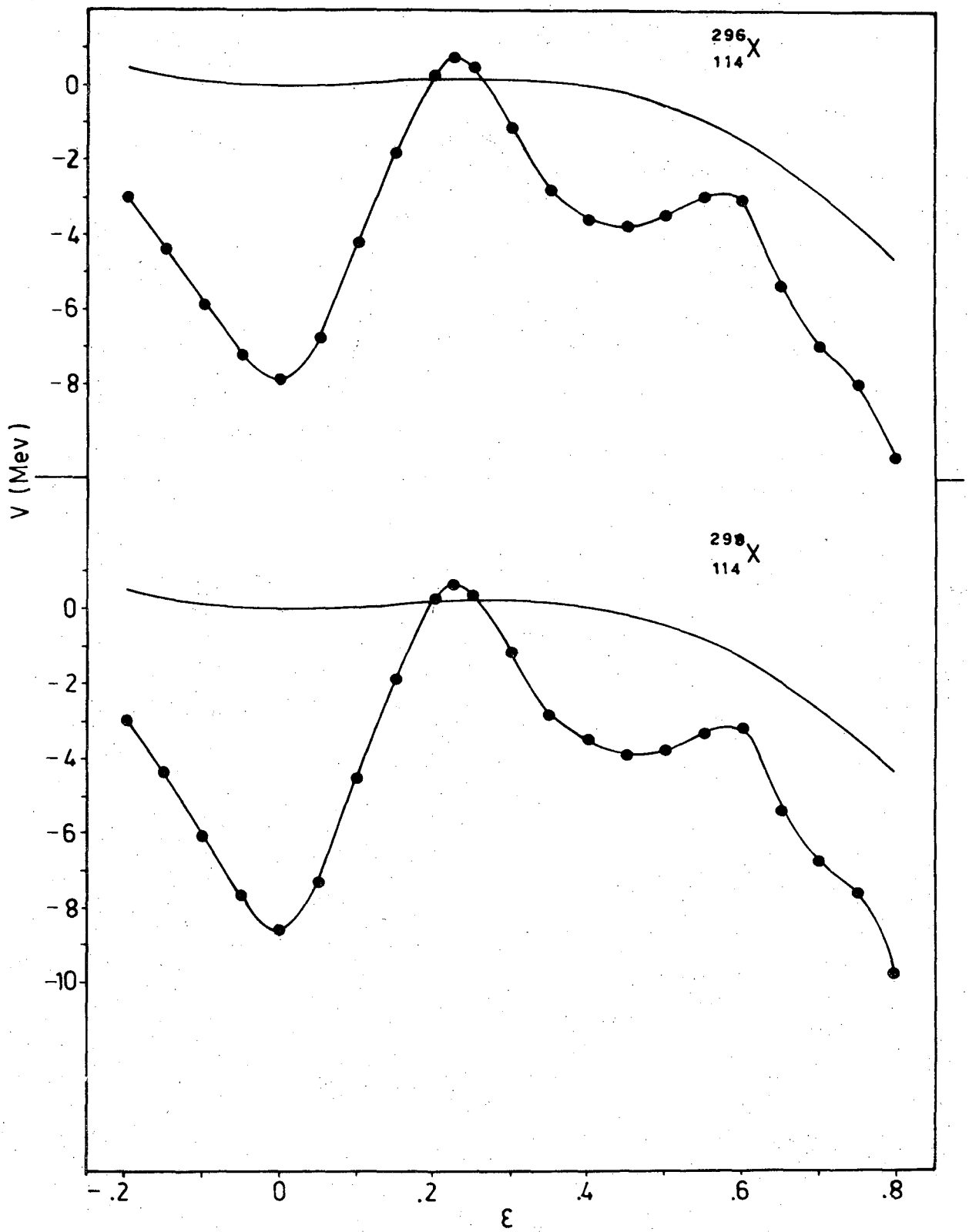

Fig. 4

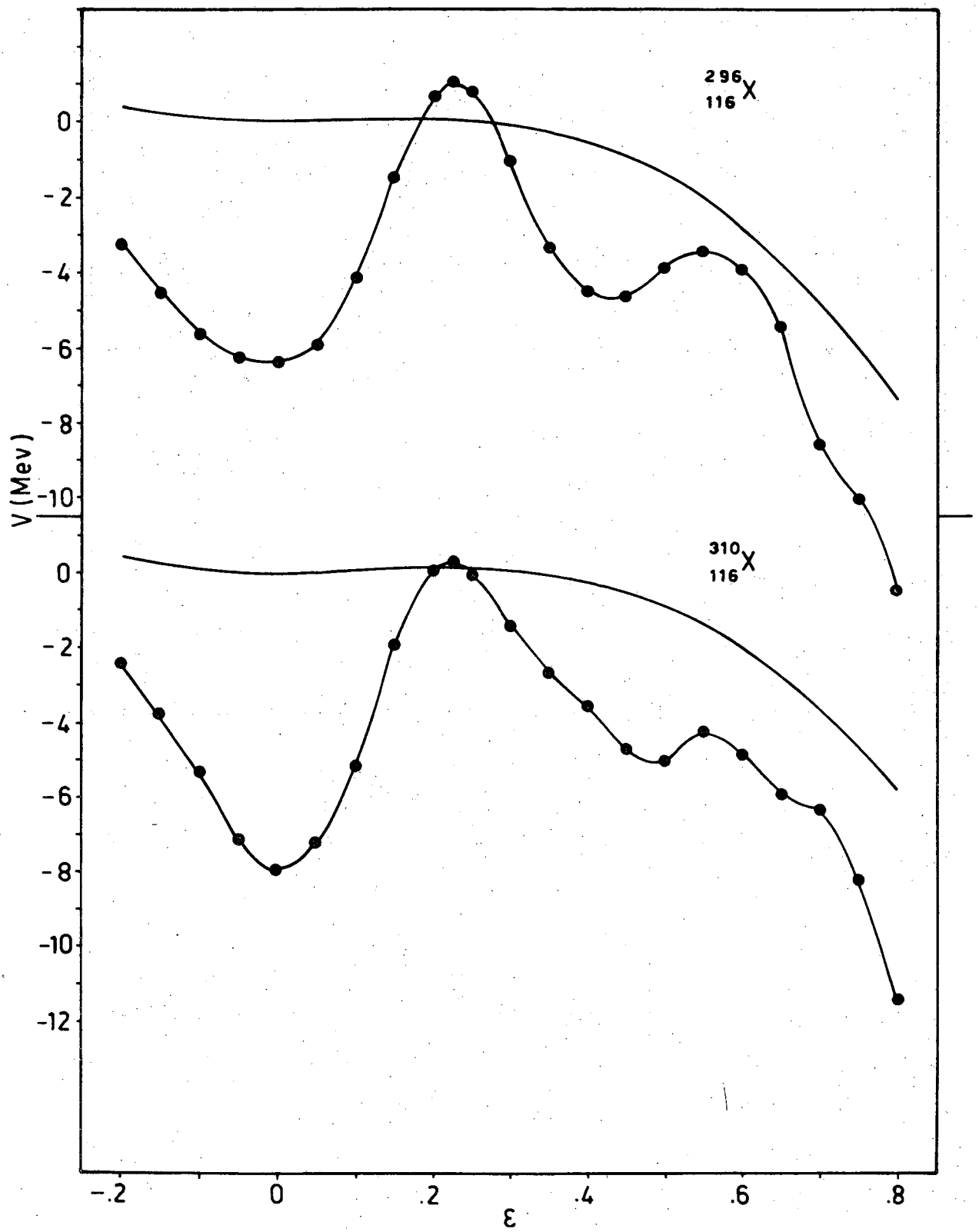

Fig. 5

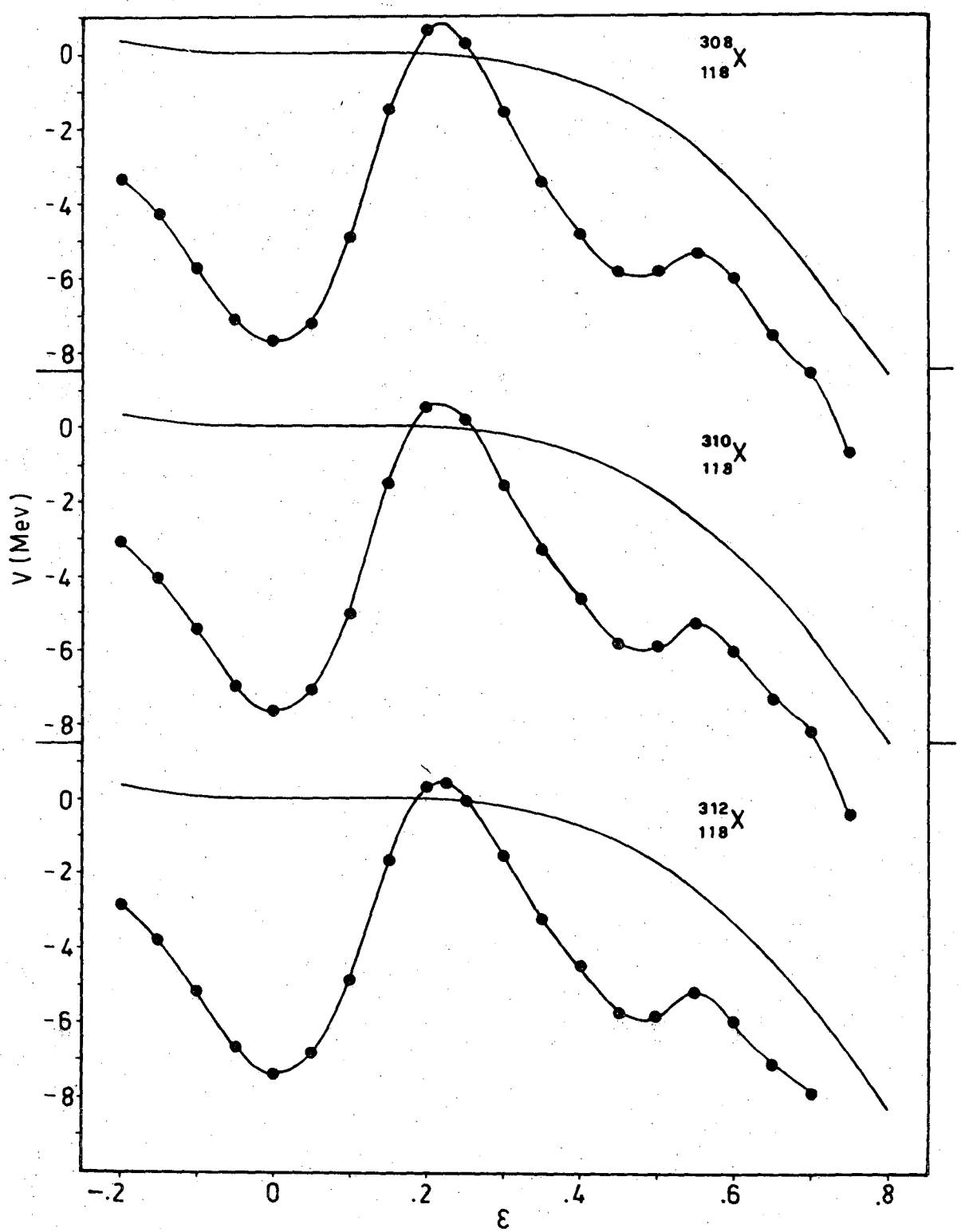

Fig. 6

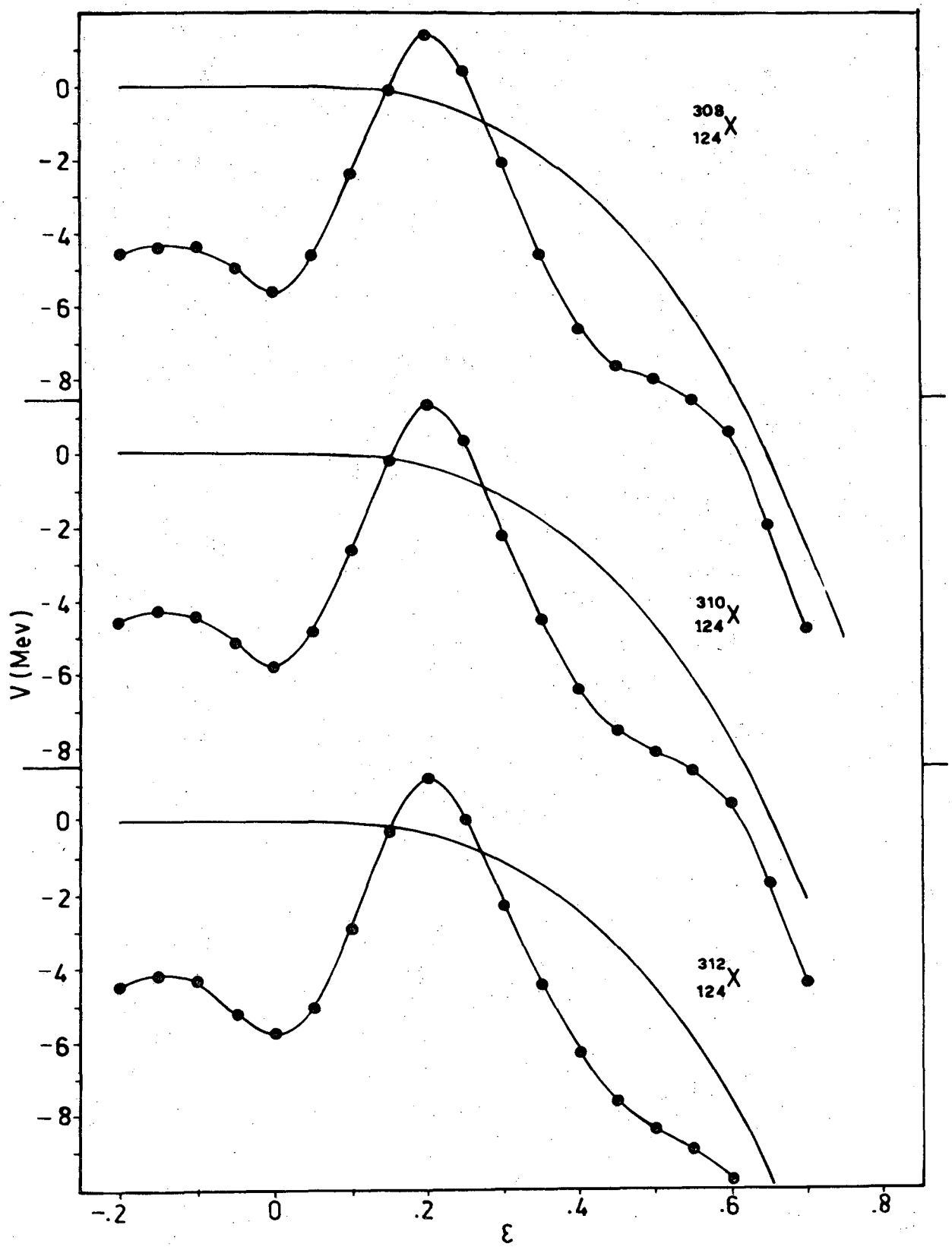

Fig. 7

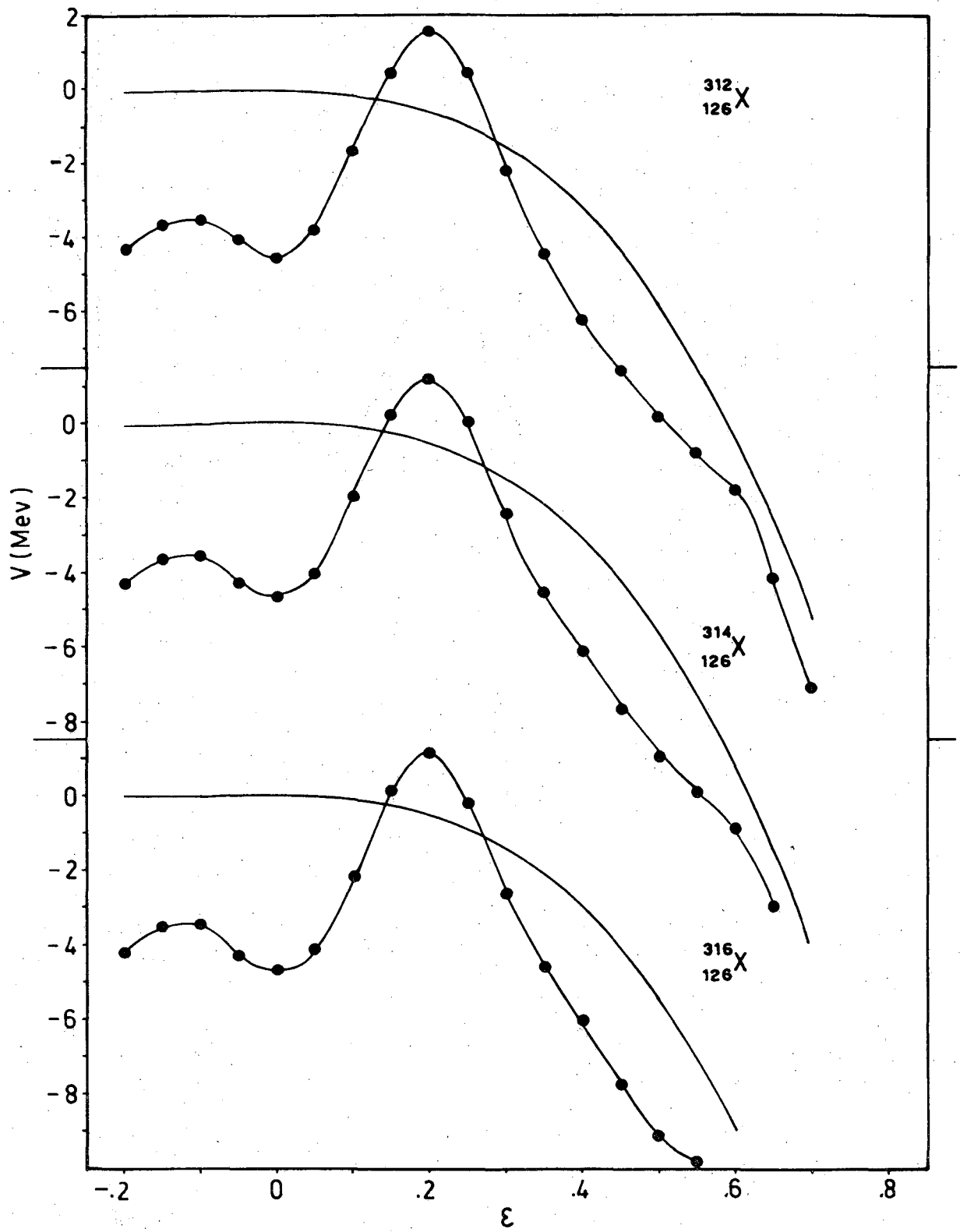

Fig. 8

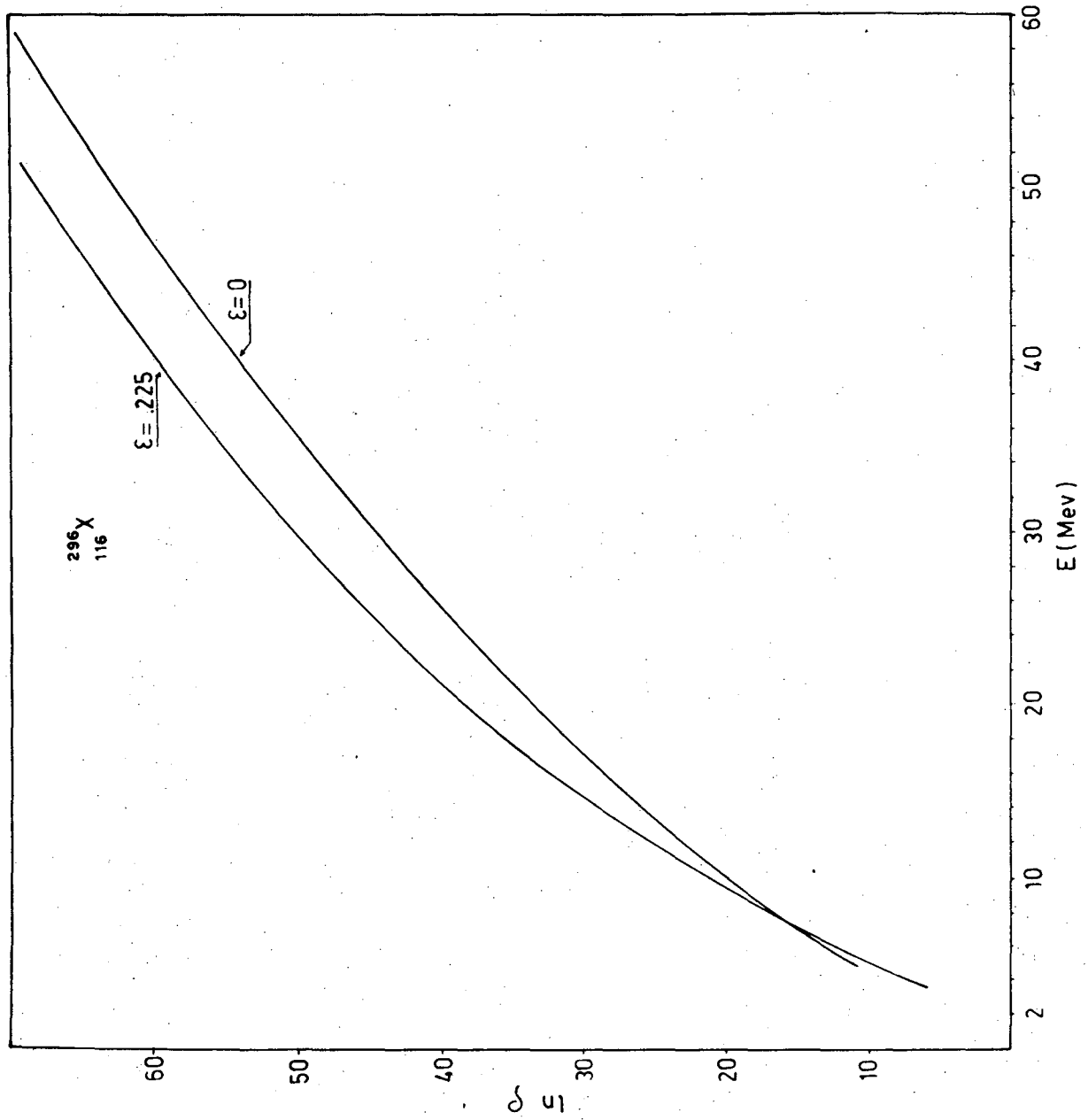

Fig. 9

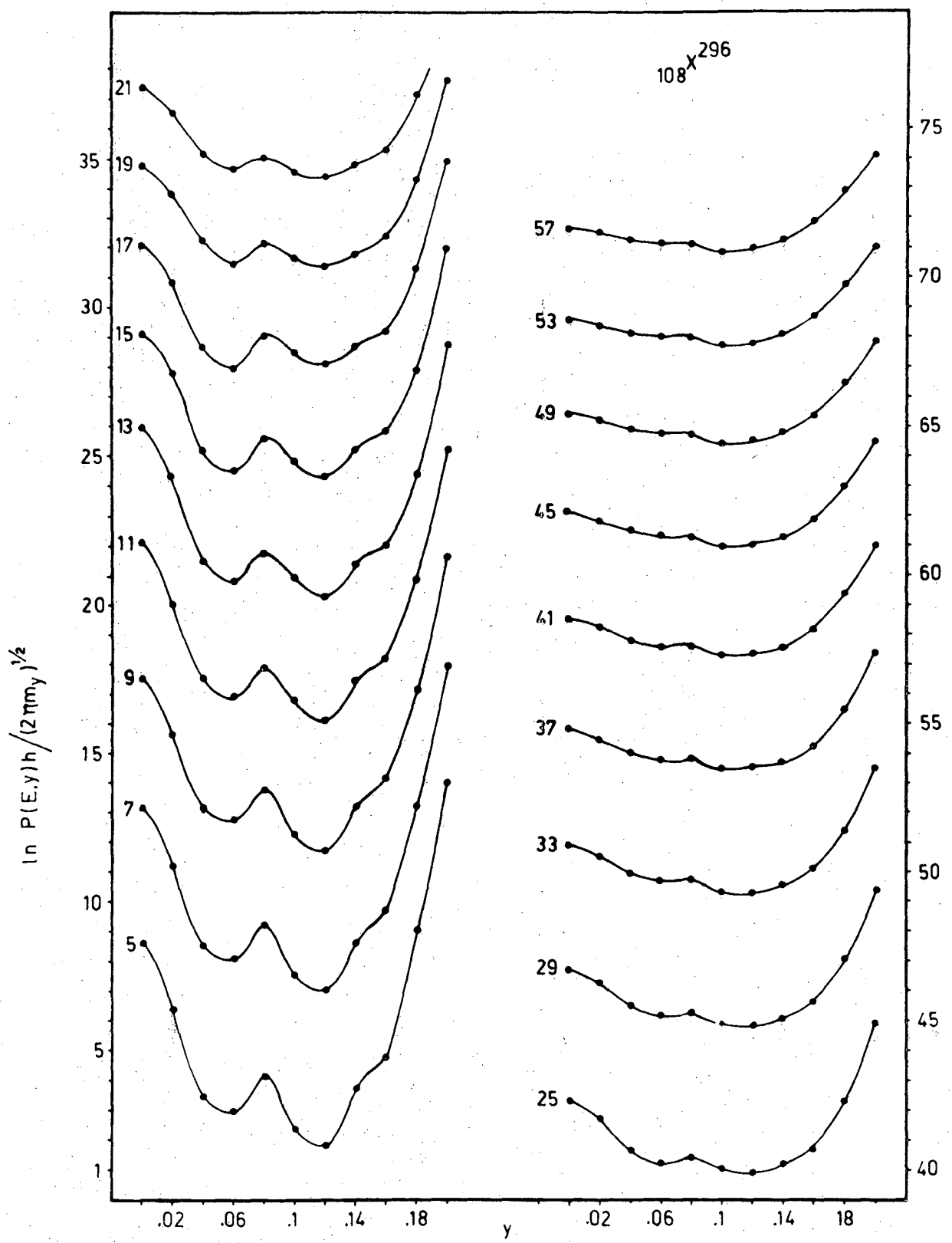
108X296
21
19
17
15
13
11
9
7
5
57
53
49
45
41
37
33
29
25
35
30
25
20
15
10
5
1
75
70
65
60
55
50
45
40
ln P(E,y)h/(2πm_y)^½
.02
.06
.1
.14
.18
y

Fig. 10

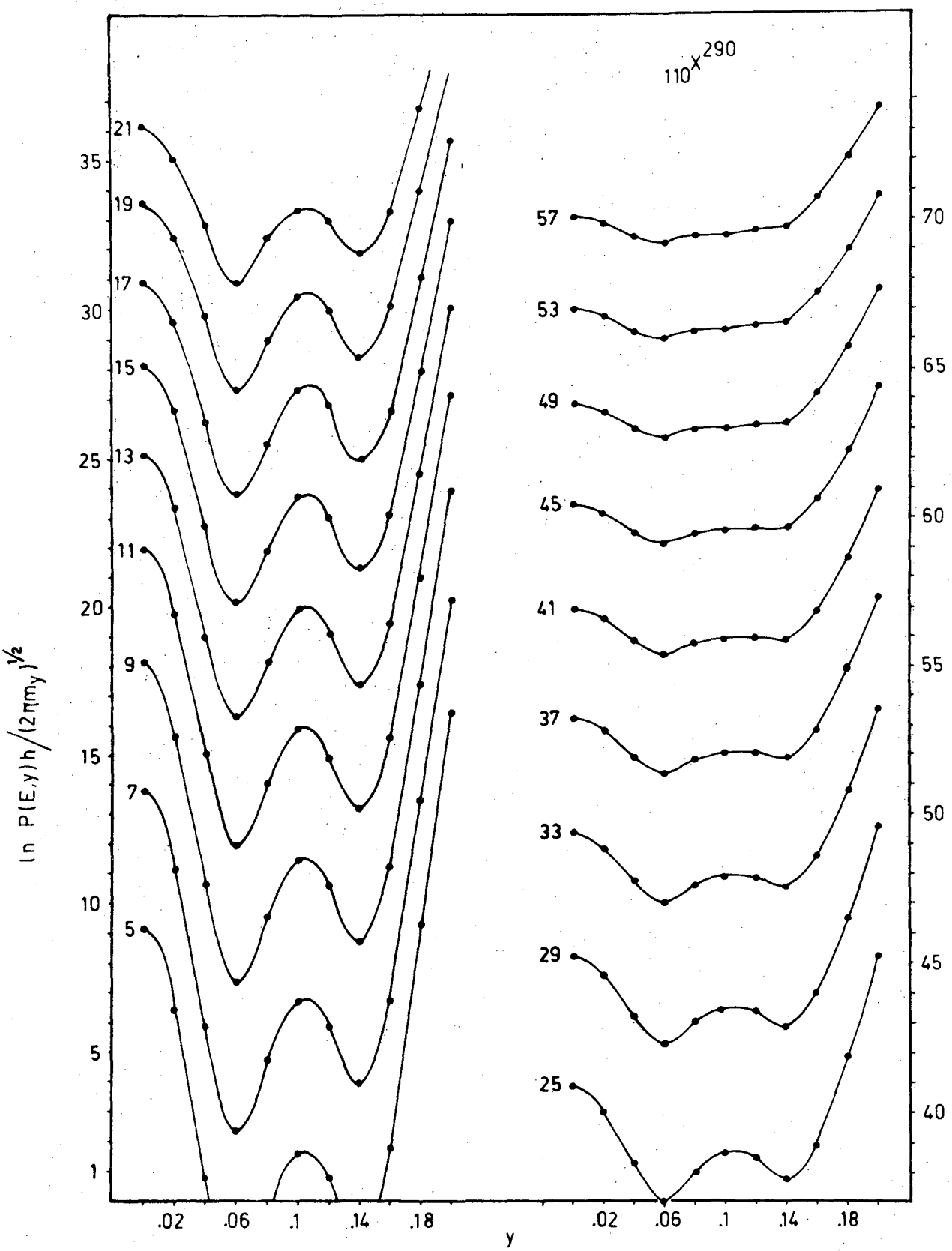
110X290
21
19
17
15
13
11
9
7
5
57
53
49
45
41
37
33
29
25
35
30
25
20
15
10
5
1
70
65
60
55
50
45
40
ln P(E,y)h/(2πm_y)^½
.02
.06
.1
.14
.18
y

Fig. 11

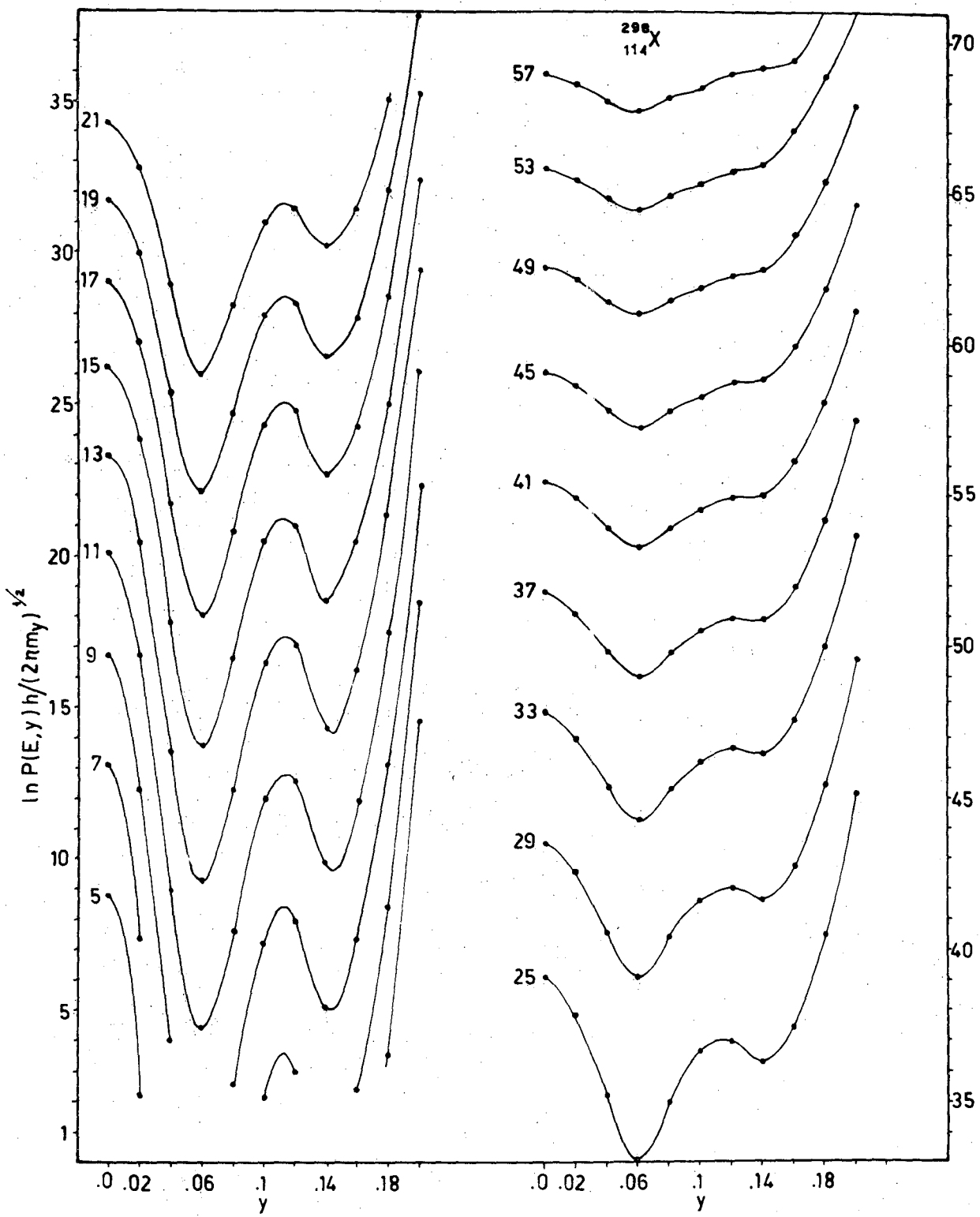

$^{298}_{114}X$
ln P(E,y) h/(2πm_y)^½
y
.0 .02 .06 .1 .14 .18
1 5 10 15 20 25 30 35
21 19 17 15 13 11 9 7 5
57 53 49 45 41 37 33 29 25
35 40 45 50 55 60 65 70

Fig. 12

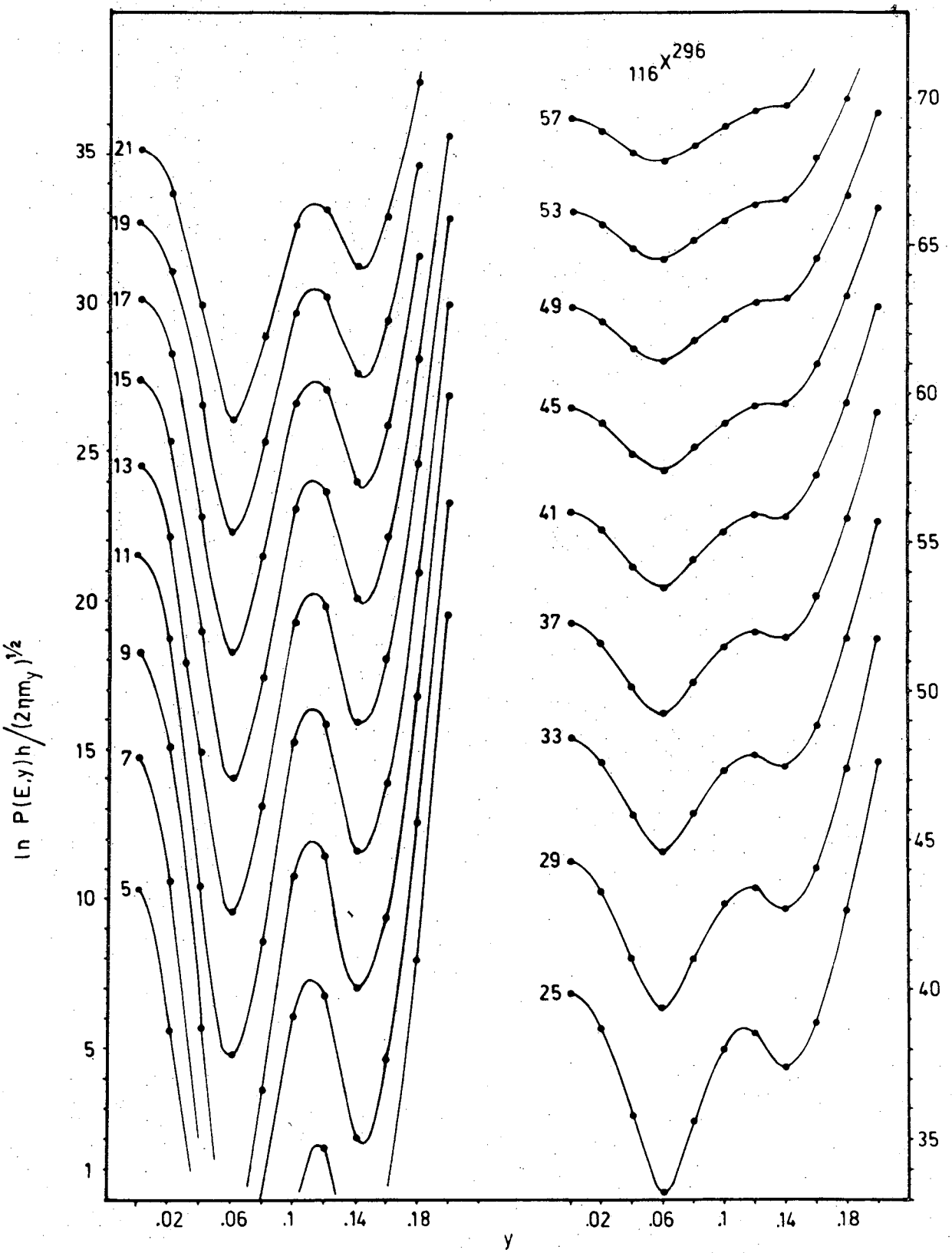
$^{116}X^{296}$
ln $P(E,y)h/(2\eta m_y)^{1/2}$
y
.02
.06
.1
.14
.18
1
5
10
15
20
25
30
35
40
45
50
55
60
65
70
5
7
9
11
13
15
17
19
21
25
29
33
37
41
45
49
53
57

Fig. 13

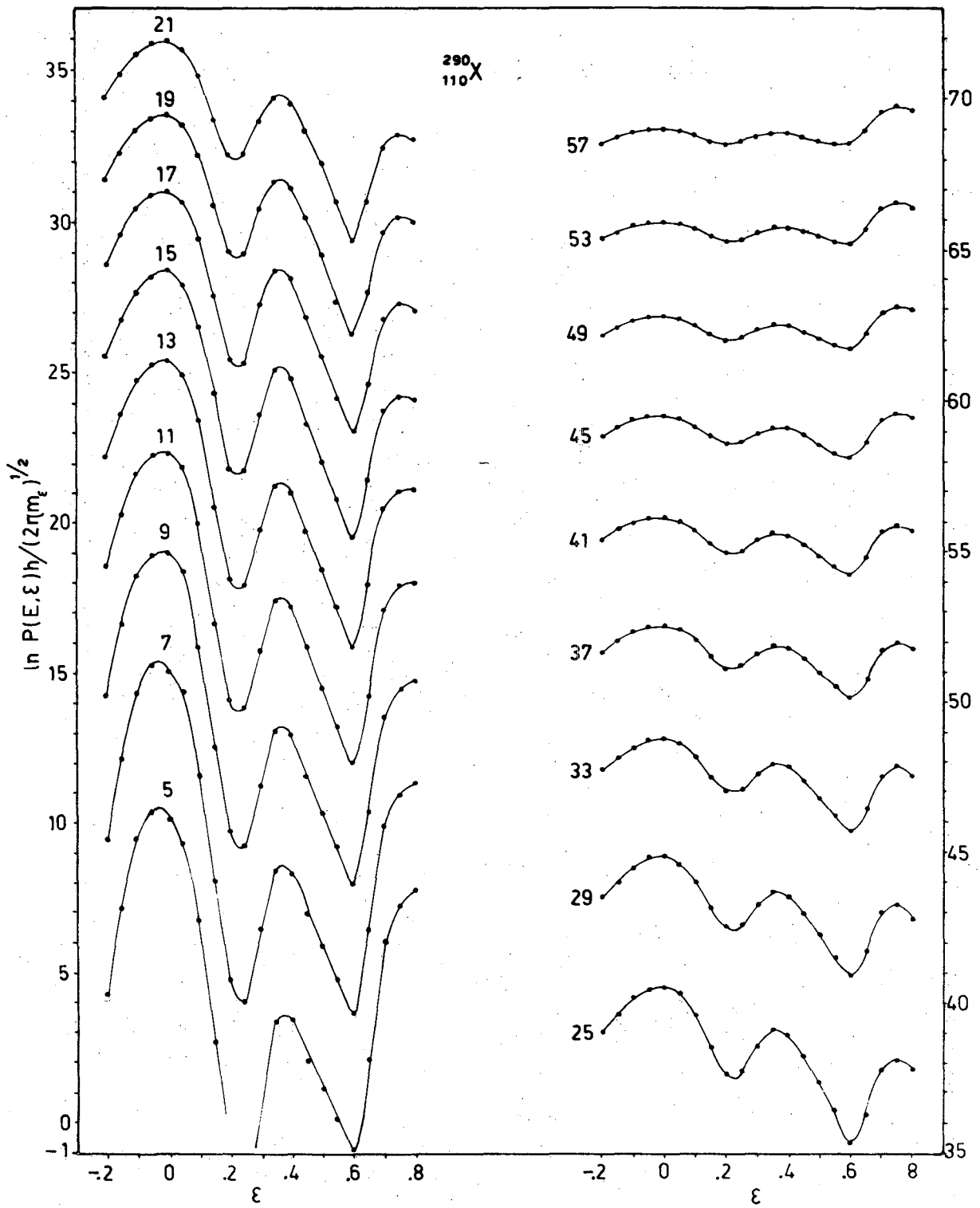

$^{290}_{110}X$
21
19
17
15
13
11
9
7
5
57
53
49
45
41
37
33
29
25
ln P(E,ε)h/(2π(m_ε)^{1/2})
ε
ε

Fig. 14

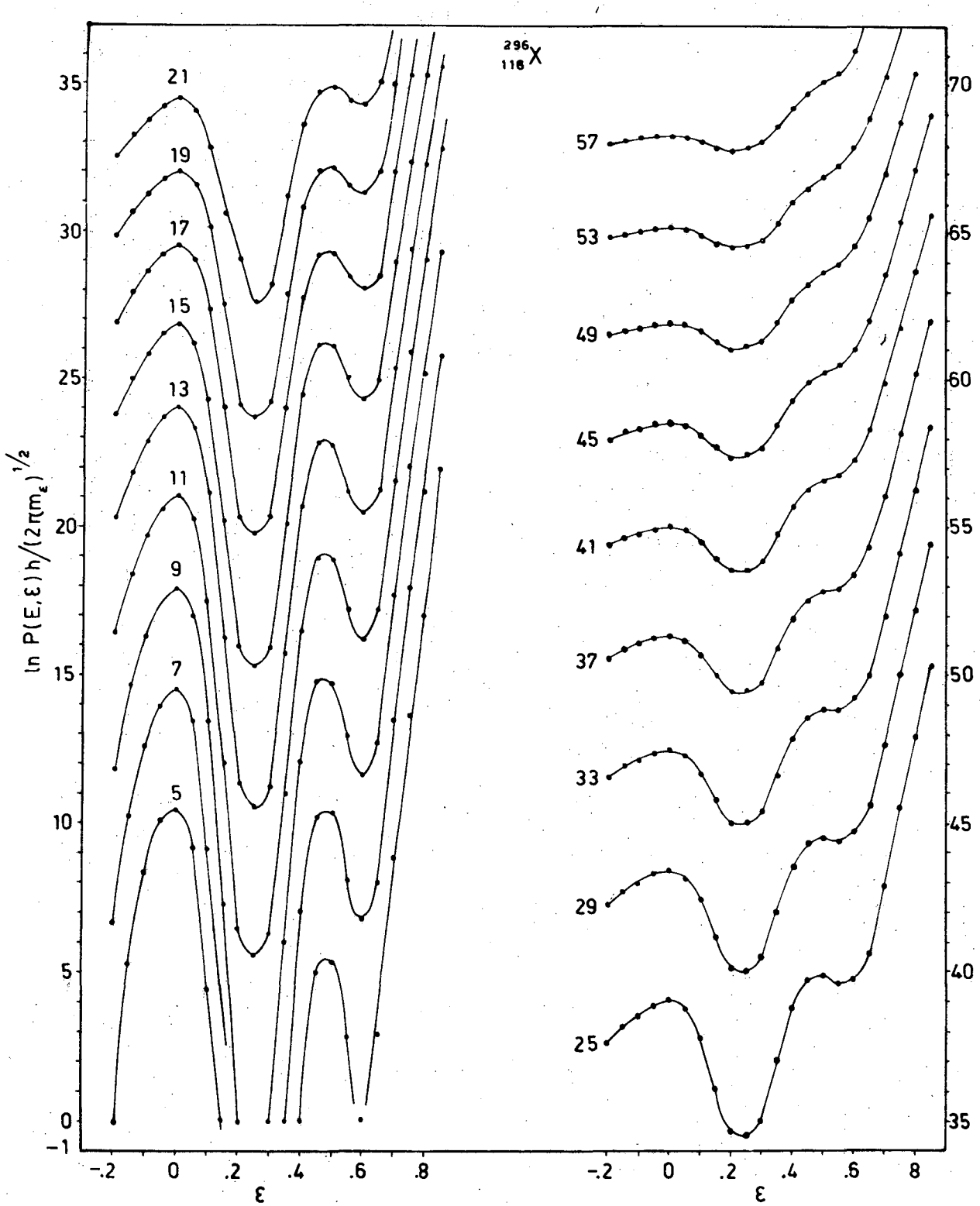
296
118 X
21
19
17
15
13
11
9
7
5
57
53
49
45
41
37
33
29
25
35
30
25
20
15
10
5
0
-1
70
65
60
55
50
45
40
35
ln P(E,ε) h/(2π(m_ε))^1/2
-.2
0
.2
.4
.6
.8
ε
-.2
0
.2
.4
.6
8
ε

Fig. 15

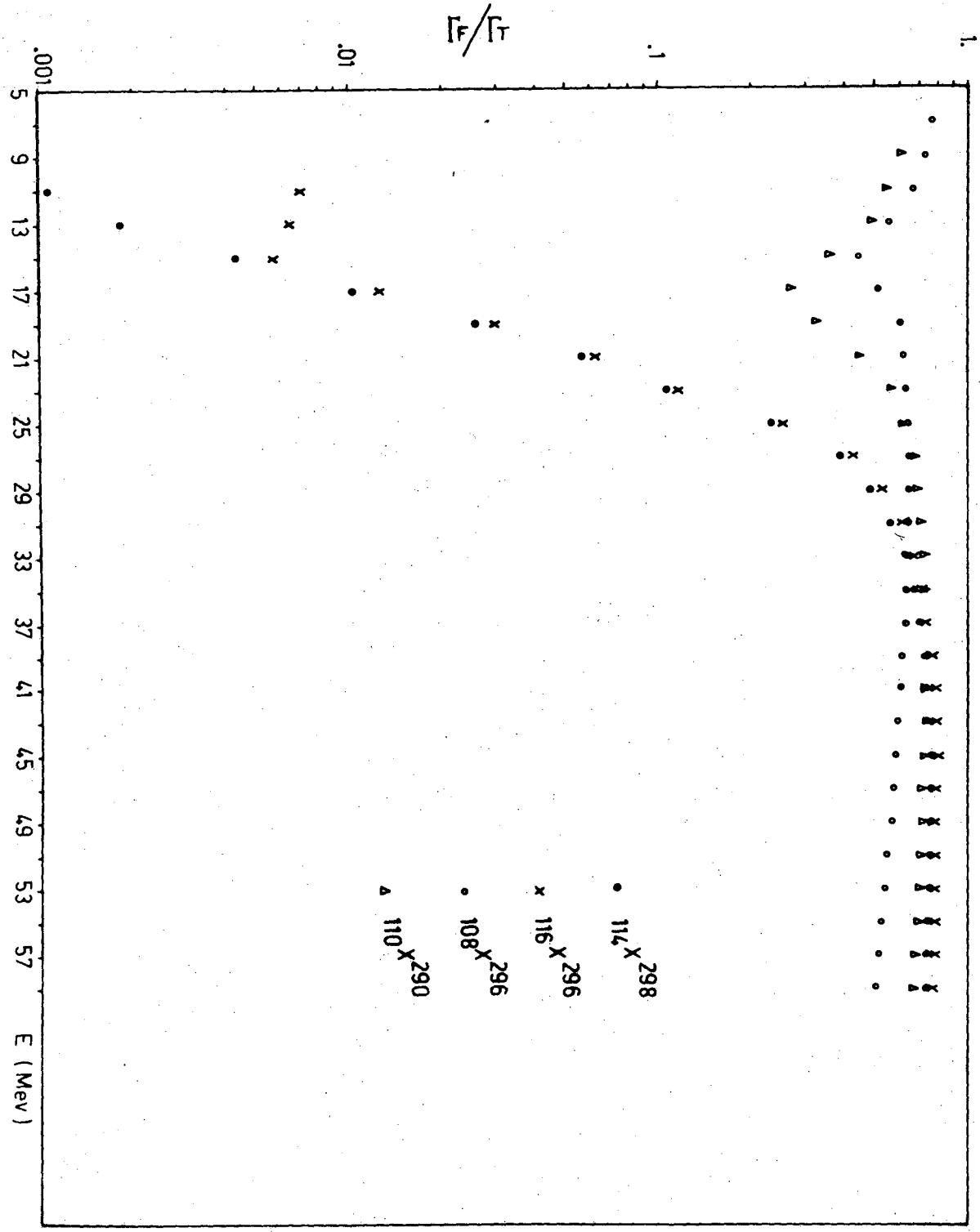
1.
.1
.01
.001
Γ_F/Γ_T
5
9
13
17
21
25
29
33
37
41
45
49
53
57
E (Mev)
114X298
116X296
108X296
110X290

Fig. 16

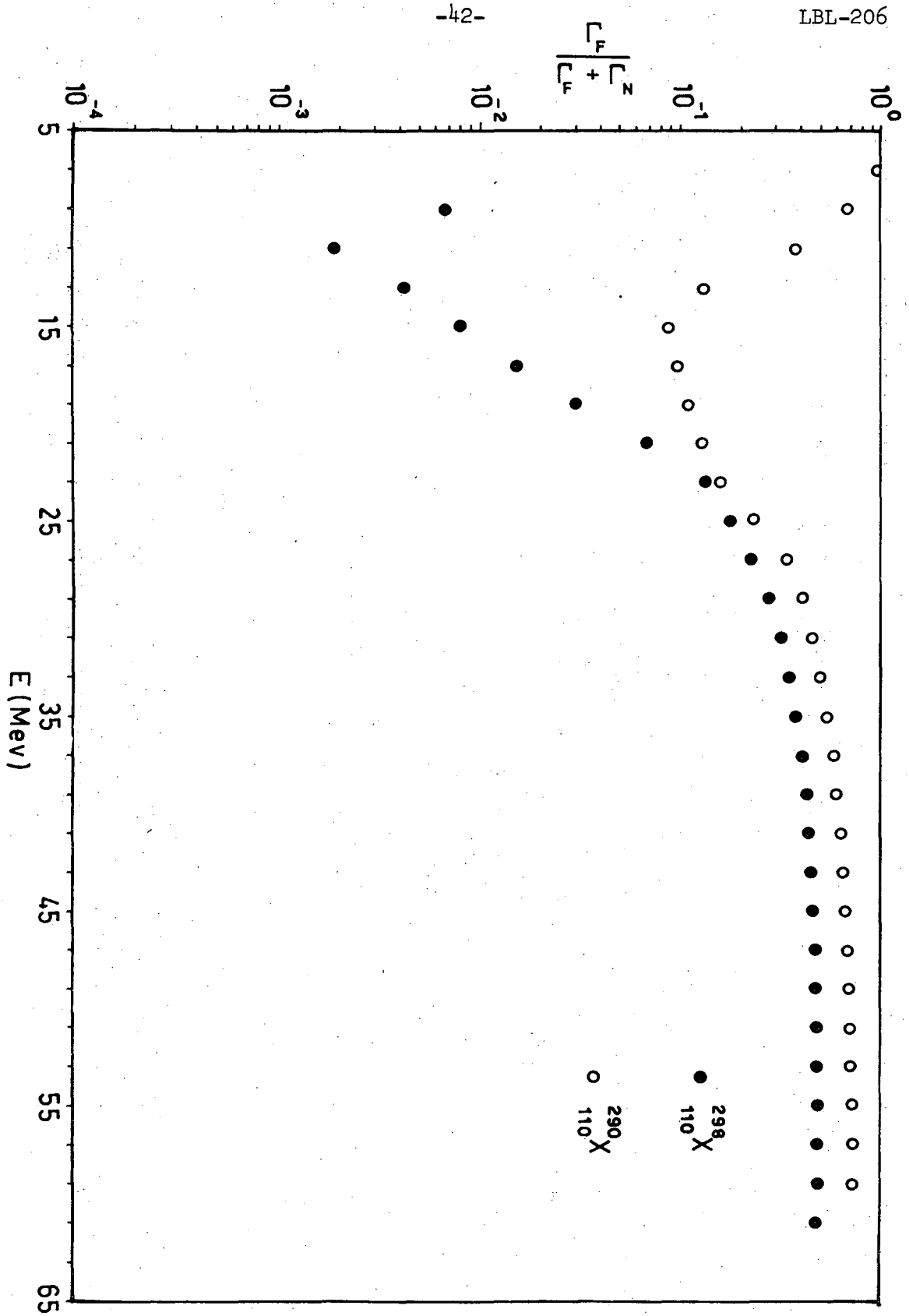
$\frac{\Gamma_F}{\Gamma_F + \Gamma_N}$
10^{0}
10^{-1}
10^{-2}
10^{-3}
10^{-4}
5
15
25
35
45
55
65
E (Mev)
$^{298}_{110}X$
$^{290}_{110}X$

Fig. 17

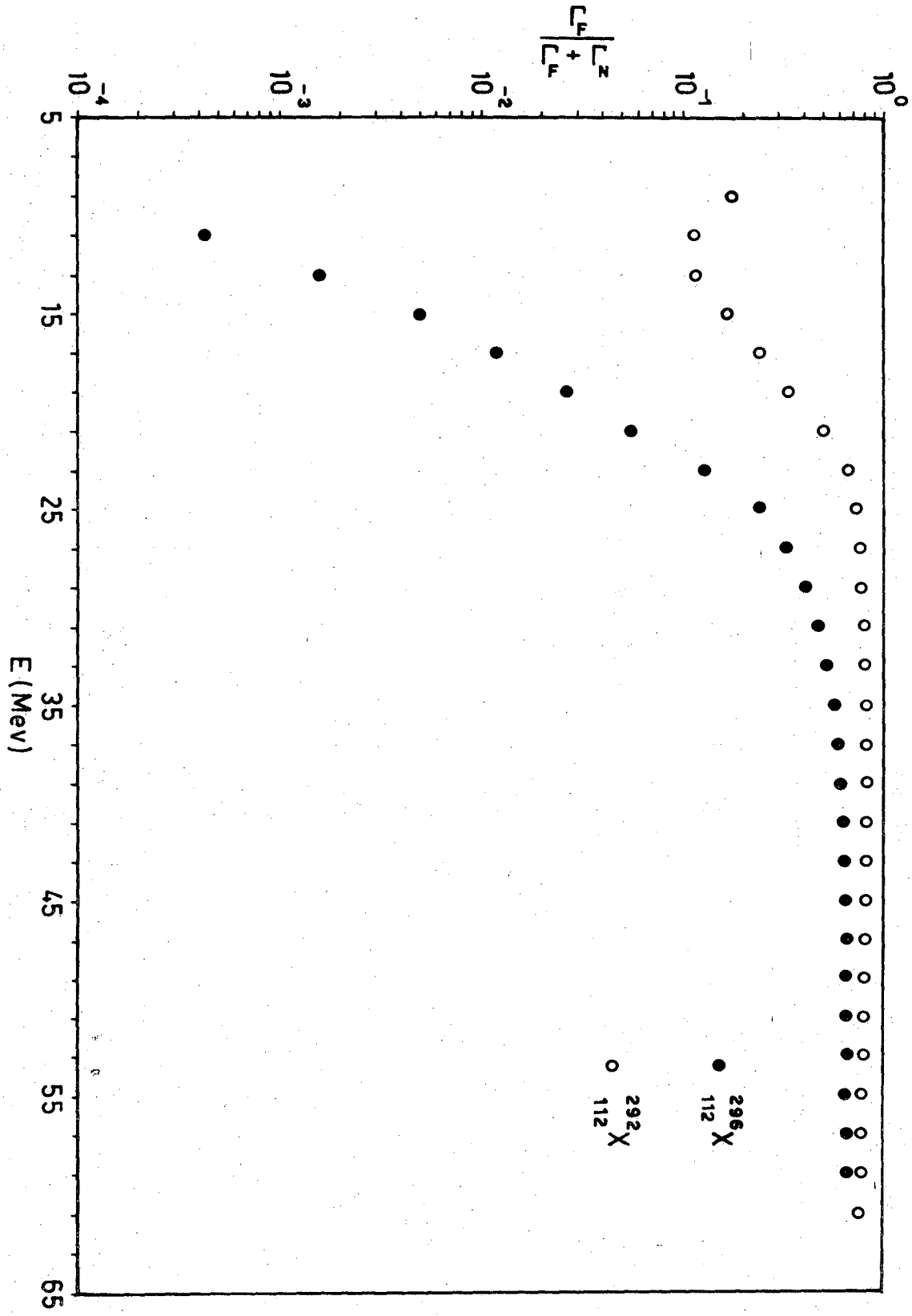
$\frac{\Gamma_F}{\Gamma_F + \Gamma_N}$
10^0
10^{-1}
10^{-2}
10^{-3}
10^{-4}
5
15
25
35
45
55
65
E (Mev)
$^{296}_{112}X$
$^{292}_{112}X$

Fig. 18

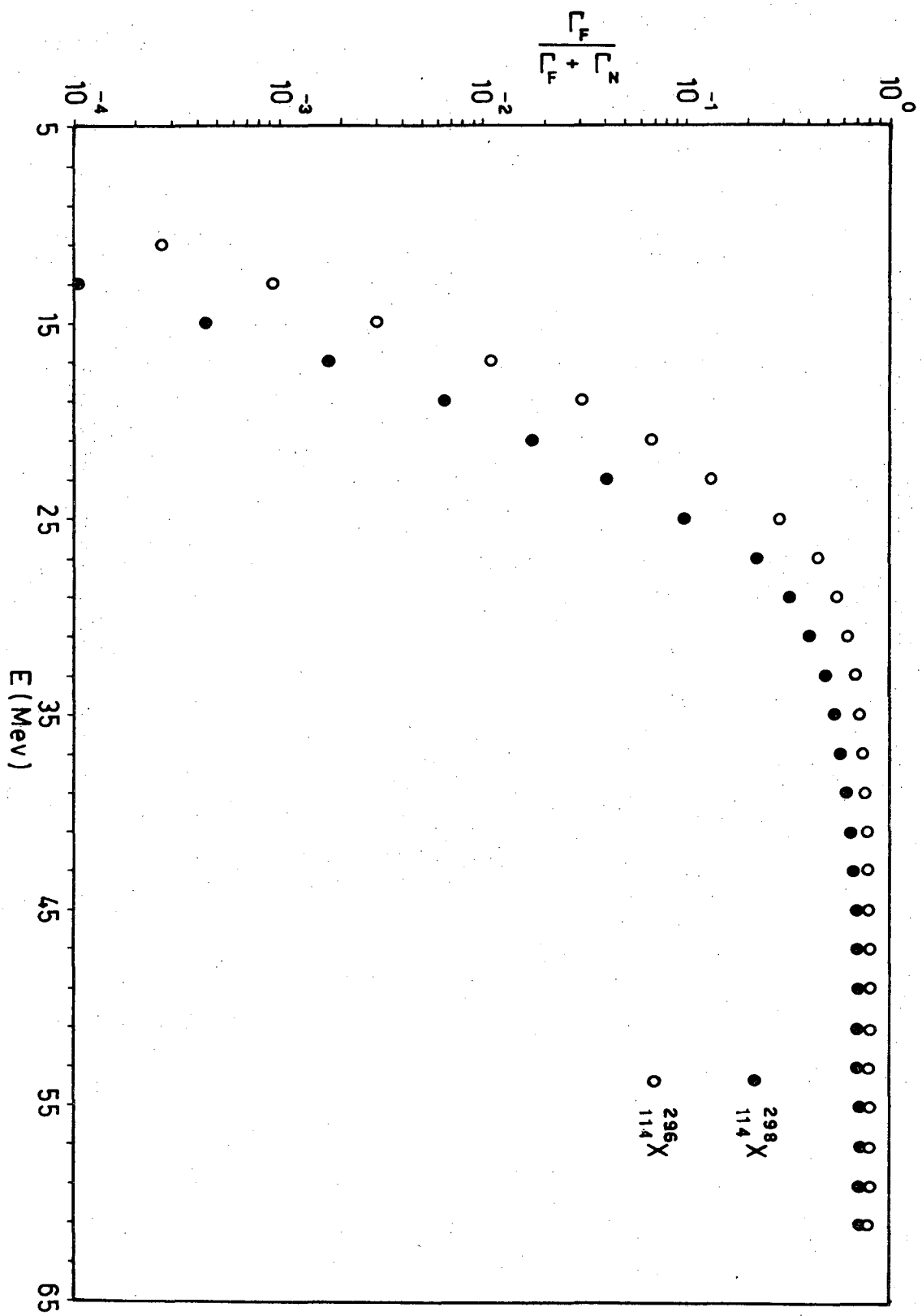
$\frac{\Gamma_F}{\Gamma_F + \Gamma_N}$
10^{0}
10^{-1}
10^{-2}
10^{-3}
10^{-4}
5
15
25
35
45
55
65
E (Mev)
$^{298}_{114}X$
$^{296}_{114}X$

Fig. 19

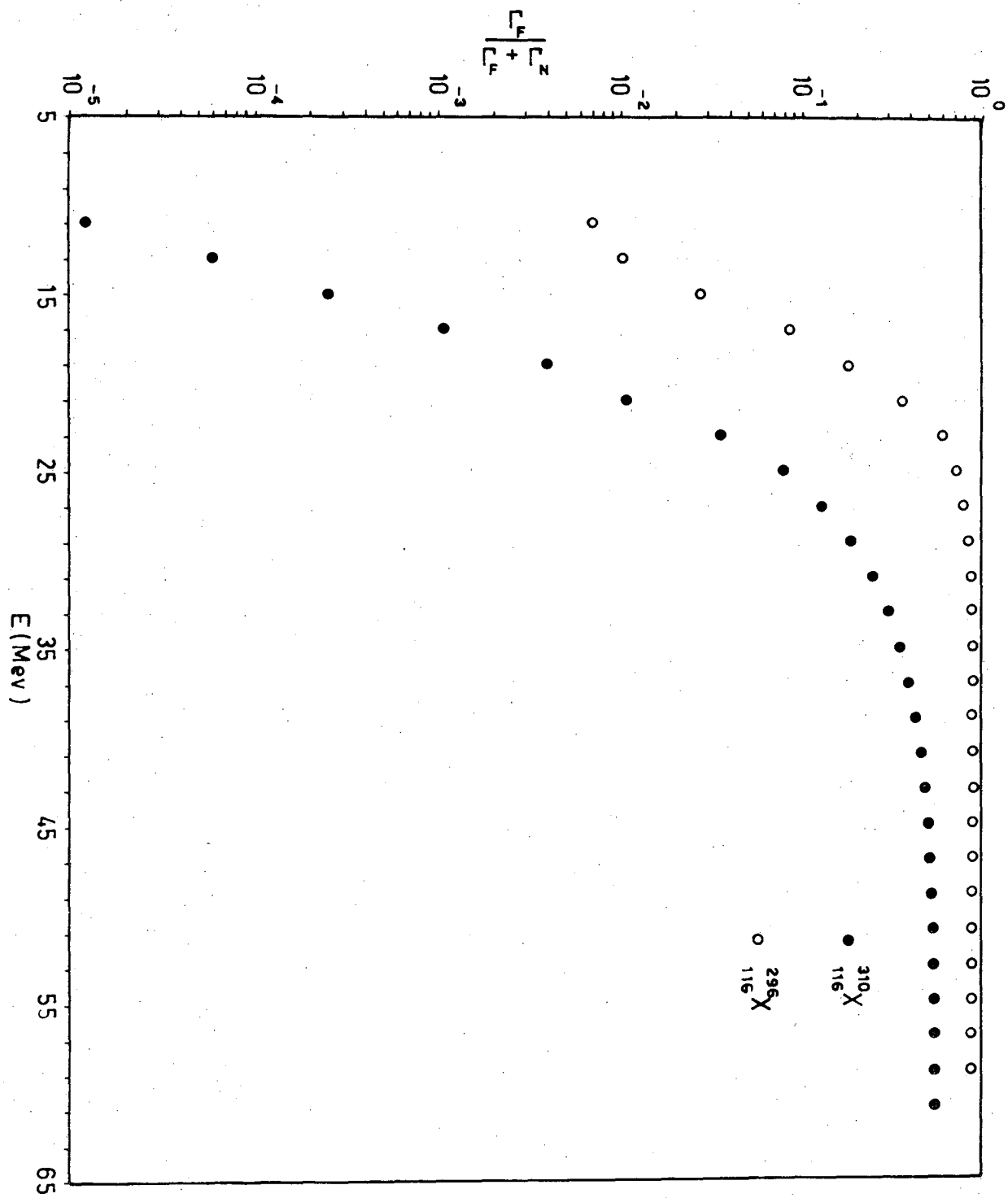
$\frac{\Gamma_F}{\Gamma_F + \Gamma_N}$
10^{0}
10^{-1}
10^{-2}
10^{-3}
10^{-4}
10^{-5}
5
15
25
35
45
55
65
E (Mev)
$^{310}_{116}X$
$^{296}_{116}X$

Fig. 20

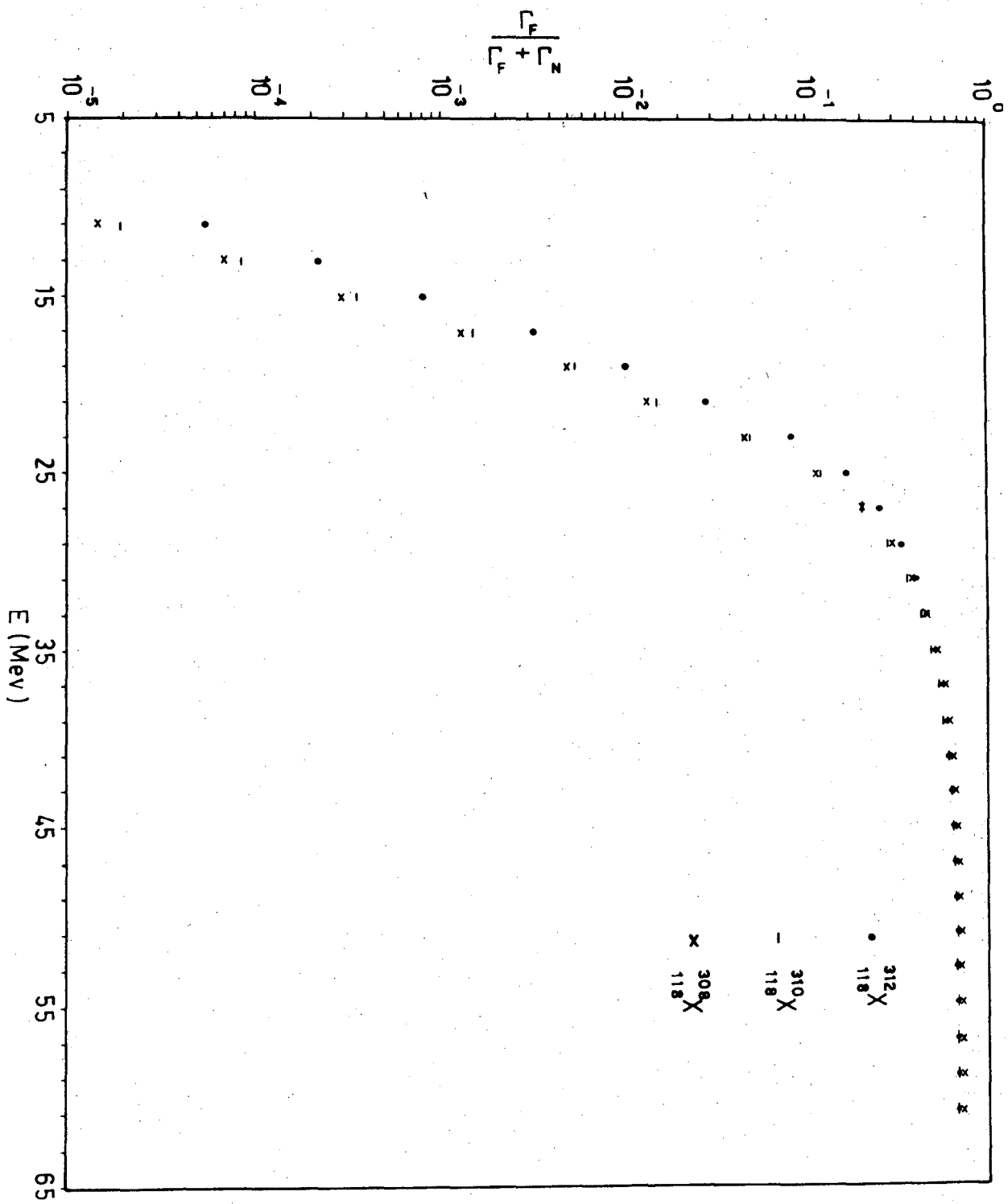
$\frac{\Gamma_F}{\Gamma_F + \Gamma_N}$
10^{0}
10^{-1}
10^{-2}
10^{-3}
10^{-4}
10^{-5}
65
55
45
35
25
15
5
E (Mev)
312
118
310
118
308
118

Fig. 21

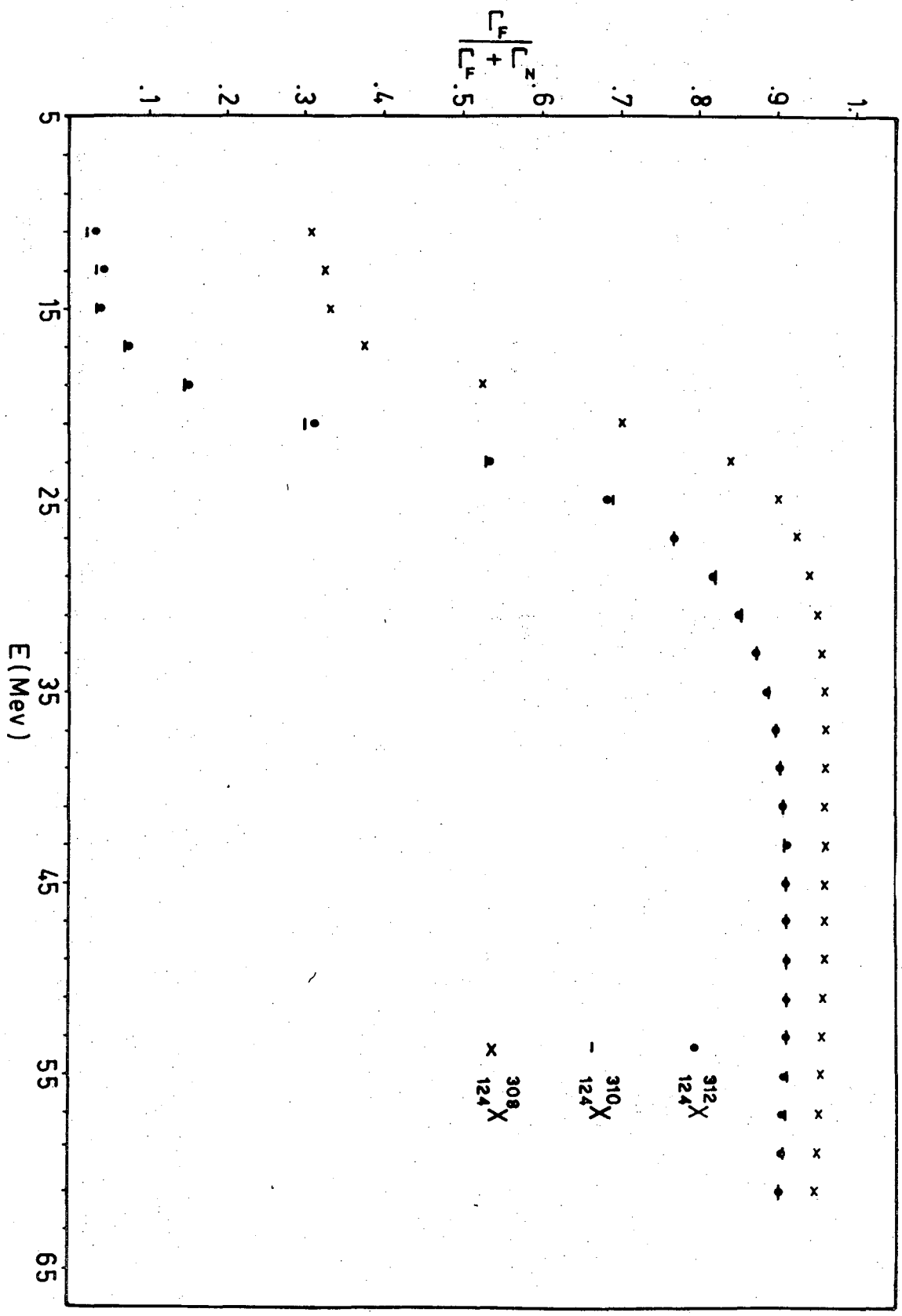
$\frac{\Gamma_F}{\Gamma_F + \Gamma_N}$
1.
.9
.8
.7
.6
.5
.4
.3
.2
.1
5
15
25
35
45
55
65
E (Mev)
312 124
310 124
308 124

Fig. 22

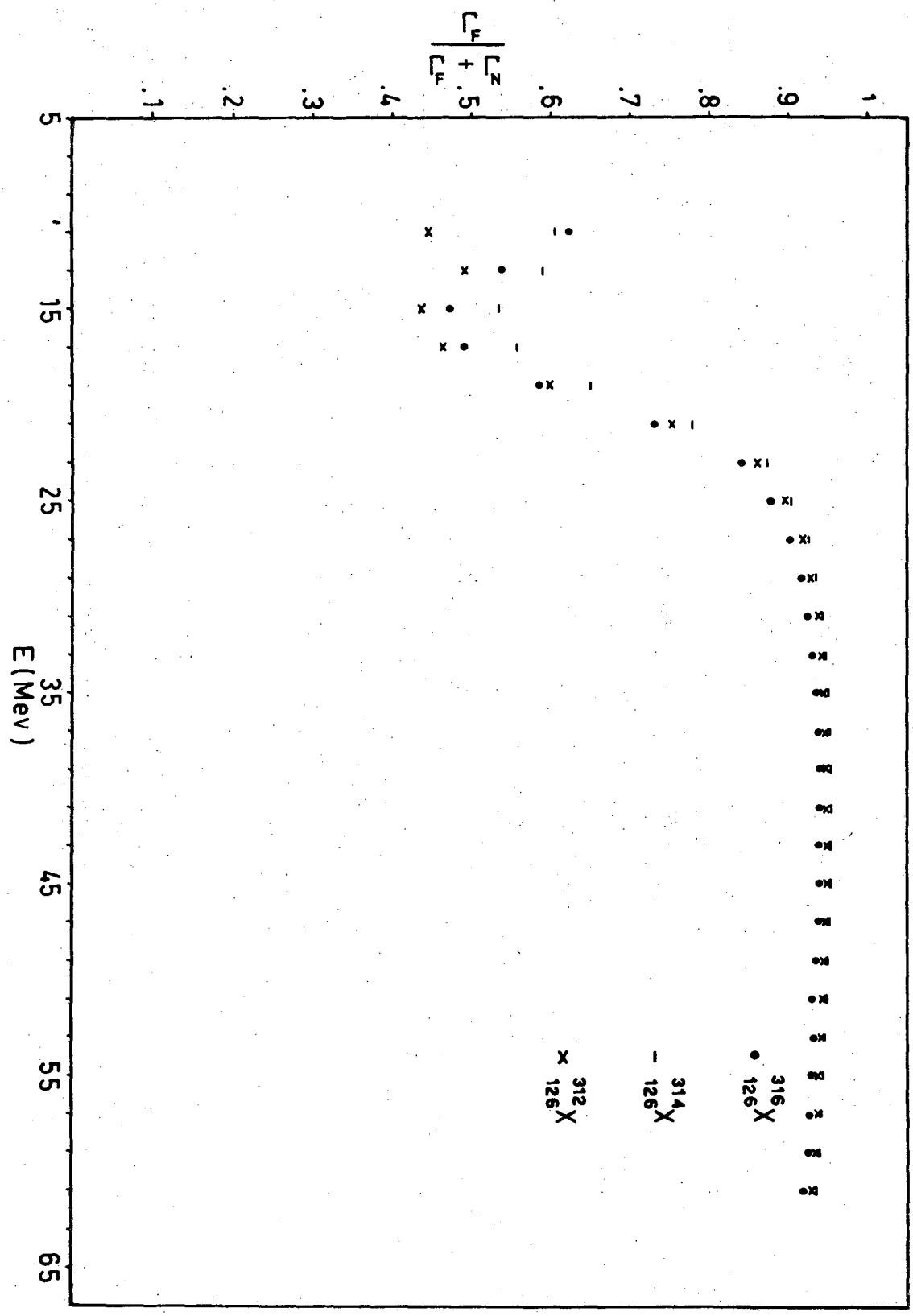
$\frac{\Gamma_F}{\Gamma_F + \Gamma_N}$
.1
.2
.3
.4
.5
.6
.7
.8
.9
1
5
15
25
35
45
55
65
E (Mev)
316
126
314
126
312
126

Fig. 23

LEGAL NOTICE

This report was prepared as an account of work sponsored by the United States Government. Neither the United States nor the United States Atomic Energy Commission, nor any of their employees, nor any of their contractors, subcontractors, or their employees, makes any warranty, express or implied, or assumes any legal liability or responsibility for the accuracy, completeness or usefulness of any information, apparatus, product or process disclosed, or represents that its use would not infringe privately owned rights.

TECHNICAL INFORMATION DIVISION
LAWRENCE BERKELEY LABORATORY
UNIVERSITY OF CALIFORNIA
BERKELEY, CALIFORNIA 94720